

# Modeling and analysis of cost-effective energy management for integrated microgrids

Abu Shufian<sup>a,\*</sup>, Nur Mohammad<sup>b</sup>

<sup>a</sup> Institute of Energy Technology, Chittagong University of Engineering & Technology, Chattogram, 4349, Bangladesh

<sup>b</sup> Department of Electrical and Electronic Engineering, Chittagong University of Engineering & Technology, Chattogram, 4349, Bangladesh

## ARTICLE INFO

### Keywords:

Microgrid  
Solar energy  
Energy storage  
Energy management system  
Prediction  
Optimization  
Heuristic  
Linear programming  
Optimal power flow  
Cost forecast

## ABSTRACT

A microgrid concept is an innovative approach for integrating hybrid and renewable energy sources into the utility grid. The uncertainties because of the intermittent nature of renewable energy resources, the load, and market price are significant challenges. In the traditional heuristic method, data is forecast but not known perfectly. Improving energy storage systems and energy management systems (EMS) development using optimization-based methods is a possible solution to improve the performance of microgrid operations. The EMS is an essential part of the distributed energy resources in the microgrid system, especially when power generation, transmission, distribution, utilization, and variable pricing are involved. This optimization process developed in this paper uses forecasted costs and loading conditions to store or sell the energy from an integrated grid battery system. Two approaches are introduced in this research work: the heuristic method using state flow (chart flow) and the optimization method based on linear programming (LP), which minimizes operation costs (savings of around 19% cost) subject to operational constraints. The LP optimization saves roughly 3.44–5.01% of excess grid energy. Several plausible outcomes of this research study simplify the comprehensive, integrated microgrid simulation for EMS optimization algorithm validation. The suggested integrated microgrid management system might be a testbed for smart grid technology research.

## 1. Introduction

Nowadays, most countries are focusing on their energy-based industrial and commercial revolutions. These developments underlay the uptake of sustainable and uninterrupted energy production, the first and fundamental element. Increasing electricity generation in various traditional ways (fossil fuel-based) sometimes leads to unsustainability. Scientists and policymakers have to think about the next generation of safer technology for human beings and the environment. Using too many fossil fuels to generate electricity is harmful to nature because of global warming. Therefore, renewable energy harness/utilization and proper economic management are prime concerns for energy safety and security. Although the renewable source is quickly expanding throughout the world, fossil fuels remain the source of the vast bulk of global energy consumption. Oil, coal, and natural gas accounted for 84% of global energy use in 2020 (Lee et al., 2012). These fossil fuels are not inexhaustible, and researchers mention that if fossil fuel burning is kept at the current rate, it is generally estimated that all fossil fuels will be depleted by 2060 (Gulagi et al., 2020). As a result, there have been few

international commitments to encourage hybrid or self-sufficient renewable generation technology. This endeavor has resulted in the spread of renewable energy production's ability to produce resilient and uninterrupted electricity from several renewable energy sources (Yang et al., 2019). The biggest challenge is securing and making safer energy generation from renewables and utilizing it with a proper and effective management system.

An integrated electrical grid is a network of linked power lines that transport energy from renewable generators to consumers. It comprises a producing station that generates electricity and substations that scale the voltage up or down for transmission or distribution. The rapid increase in the utilization of electrical energy urges low-cost, environment-friendly electricity generation, transmission, and distribution in today's world. Therefore, smart grid technology has been introduced in many parts of the world, which gives advanced automation, communication, and information technology to the power system that can monitor power flows from sites of supply to sites of consumption in real-time or near real-time and manage the flow or reduce the demand to match generation. Besides, the microgrid concept has become efficient and effective for isolated (islands) areas, which gives a collection of

\* Corresponding author.

E-mail addresses: [shufian.eee@gmail.com](mailto:shufian.eee@gmail.com) (A. Shufian), [nur.mohammad@cuet.ac.bd](mailto:nur.mohammad@cuet.ac.bd) (N. Mohammad).

<https://doi.org/10.1016/j.clet.2022.100508>

Received 22 January 2022; Received in revised form 18 April 2022; Accepted 7 May 2022

Available online 13 May 2022

2666-7908/© 2022 The Author(s). Published by Elsevier Ltd. This is an open access article under the CC BY-NC-ND license (<http://creativecommons.org/licenses/by-nc-nd/4.0/>).

Nomenclature	
<b>Acronyms</b>	
PV	Photovoltaic
EMS	Energy Management System
ESS	Energy Storage Systems
DG	Distributed Generation
DER	Distributed Energy Resources
BIPV	Building Integrated Photovoltaics
STC	Standard Test Conditions
SCADA	Supervisory Control and Data Acquisition
NPC	Net Present Cost
COE	Cost of Energy
LCOE	Levelized Cost of Electricity
SoC	State of charge
DoD	Depth of discharge
LP	Linear Program Optimization
<b>Symbols</b>	
$C_{PV,i}$	Cost of each solar system generation unit
$I_{Batt.char(DC)}$	Battery charging current
$H_T$	Total Horizontal irradiance on PV array plane (Wh/m <sup>2</sup> )
$G_{STC}$	Global irradiance at STC (W/m <sup>2</sup> )
$a, b, c, d, e$	Different microgrid components approx. size
$f_1, f_2, f_3$	Different microgrid components approx. Weights
$emis, GHG$	Amount of Greenhouse Gas (GHG) e.g., CO <sub>2</sub> , CO, etc. emitted by the microgrid
$C_{total,year}$	Yearly Total Cost (USD)
$P_{total,def}$	Total deferrable load
$E_{grid,sales}$	Yearly energy sold to the grid
$C_{RF}$	Capital recovery factor
$i$	Yearly interest rate
$C_{Batt(min)}$	Minimum charging capacity of the battery bank
$P_{in}$	Input power
$P_{max}$	Output maximum Power
$E_A$	PV Array's DC energy output (kWh)
$P_{load}$	Load or output power (W)
$P_{PV(total)}$	Rated/installed capacity of the integrated solar PV plant
$V_{DC}$	DC or Battery voltage (nominal) (V)
$t$	Backup duration or time in hours
$I_{DC}$	DC current (A)
$E_{PV(AC)}$	Energy generated and injected into grid (kWh)
$It$	Cost of initial investment
$(O\&M)_t$	Yearly (t) operation and maintenance expenditure
$r$	Discount rate (%)
$E_t$	Yearly (t) electrical energy generated (kWh)
$n$	Yearly (t) lifetime of PV system
$P_{nominal}$	Nominal power at STC
$Y_A$	Array Yield (h/d)
$Y_R$	Reference Yield (h/d)
$N_{Batt(max)}$	Maximum battery banks required
$N_{Batt(min)}$	Minimum battery banks required
$V_{load(max)}$	Maximum load voltage tolerance (%)
$V_{load(min)}$	Minimum load voltage tolerance (%)
$V_{eodv}$	End of discharge voltage
$P_{PVG,i}$	Quantity of power produced when the cost of each solar system production unit is kept as low as possible
$E_{DC}$	Total designed energy over autonomy (VAh)
$k_{af}$	Battery Aging Factor (%)
$k_{tef}$	Temperature Correction Factor (%)
$k_{crt}$	Capacity Rating Factor (%)
$k_{mdod}$	Maximum depth of Discharge (%)
$k_{sc}$	System Efficiency (%)

interconnected loads and dispersed energy resources (solar, wind energy, or other renewables) that operate as a single controlled entity in reference to the grid. A microgrid may connect to the grid and disconnect from it, allowing it to function in grid-connected and island modes without any significant changes (Singh and Lather, 2021). The primary issues are uninterrupted power balancing from generation to demand-side, advanced operation, monitoring, and energy management. Hence, the energy management system (EMS) is referred to as an intelligent control system designed to reduce energy consumption, improve the utilization of the grid system, predict electrical system performance, increase reliability, advance demand-side management, provide accurate forecast information for renewable energy storage, and optimize energy usage to reduce cost. It provides optimum information for transmission operators with greater insight into transmission networks and sub-transmission power flow paths, with the capability to monitor them either as a standalone/island system or as a fully integrated microgrid. For state estimation analysis, load flow, power flow, fault calculation, energy storage, contingency analysis, performance indices, optimal topology change, and voltage stability applications, EMS allows utilities to visualize better, operate, optimize, and maintain transmission and sub-transmission networks.

There are three distinct EMS techniques available: on-grid, off-grid, and hybrid EMS. In both on-grid and off-grid EMS, only one dependent EMS unit delivers functional analysis and control info on all distributed energy resources inside microgrids. Although, the generation balance and demand-side management of the on-grid and off-grid are more complicated because of their dependence on various control and communication mechanisms. Furthermore, on-grid and off-grid management have a single point of failure, and a problem in an on-grid unit would bring the whole system to collapse (Sachs and Sawodny, 2016).

So, the EMS in energy conversion, generation, and energy storage must be sustainable and efficient. Besides, the integrated EMS of hybrid microgrids has many advantages over on-grid and off-grid EMS. The integrated microgrid's numerous control systems ensure efficient power transmission. As a result of its ability to overcome the limits of both on-grid and off-grid EMS, it is gaining appeal. The quick forecast of energy scheduling with generation to load balance is one of the significant benefits of integrated microgrid EMS (Bui et al., 2018). In the integrated EMS, the microgrid power production planning model and load forecast model are always independently maintained and seldom in synchronism. A consistent user interface also makes the transition from planning to operations of information regarding power system management much more straightforward. The intermittent renewable energy-producing units, conversion units, transmission units, and the behavior of different loads at various points in the microgrid (Sahoo et al., 2018) all influence the integrated EMS design (Michaelson et al., 2017); this necessitates a great deal of research and technical attention in this sector.

An integrated microgrid system has gotten much attention in the last decade, and it has been used in a variety of places, including residential areas, academic campuses, commercial areas, military sites, industrial locations, and distant islands (da Silva et al., 2020). It can promote high penetration of distributed energy resources, increase energy efficiency, and improve grid resilience and dependability as one of the essential components of the smart distribution grid. Many academics have been drawn to the optimal functioning of EMS through the lowering of power production costs, utilizing the maximum energy generation, effective demand-side management, and market-clearing prices through the greater usage of the renewable energy-based microgrid (Tabar et al., 2018). Many experimental studies are focused on building distributed

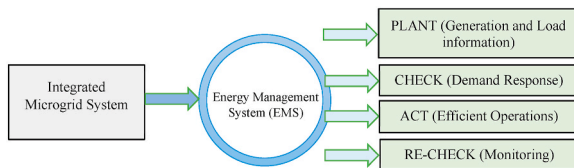


Fig. 1. Energy management system (EMS) basic feedback diagram.

energy resources and integrated microgrid optimization-based EMS systems that employ classical heuristic methods to govern integrated microgrid operation (Bellido et al., 2018). This technique requires time to adapt to the microgrid's stability, control system robustness, and operational economics. Traditional heuristic approaches cannot simply be managed up to a medium-sized or large-scale integrated microgrid because each distributed energy resource must be adequately developed and operated for stability and economic analysis (Aghdam et al., 2018). Optimization-based programming (Rabiee et al., 2018) and artificial intelligence EMS (Li et al., 2021) has gotten much attention in the field of integrated microgrid control and economic analysis in recent years. Such control techniques are generally straightforward for medium-sized or large microgrids. In 2013, an intelligent EMS for a microgrid was presented, which uses artificial intelligence and multi-objective optimization methods based on linear programming to decrease the operating cost and environmental effect of a microgrid (Chaouachi et al., 2013). With the help of a multiperiod artificial bee colony combined with the Markov chain method, an optimal EMS is proposed for islanded microgrids in 2015 which is quite cost-effective (Marzband et al., 2017). Researchers suggested a mix-mode energy management strategy in 2016, focusing on battery size to keep the microgrid running at the lowest feasible cost (Sukumar et al., 2017). For optimization, linear programming and mixed-integer linear programming are utilized. The particle swarm optimization formula is used to find the best energy capacity of battery energy storage in kWh for battery size reasons.

In 2017, some researchers have suggested an optimally scheduled hybrid AC/DC microgrid generation EMS system, which minimizes the islanded microgrid operational cost for various DG units (Nagapurkar and Smith, 2019). This system was run by receiving and sending forecast data to DG units to ensure optimum power each time. Besides, based on a regrouping particle swarm optimization energy management formula for economic operation is proposed for an industrial microgrid (Gomes et al., 2019). This system is also cost-efficient for both isolated and grid-connected loads. In 2018, comparative and critical research on decision-making techniques for microgrid energy management systems, as well as their solution approaches, will be conducted (Zia et al., 2018). There are various uncertainty quantification methods of EMS discussed which are cost-effective implementation of microgrid EMS. For the installation of renewable energy microgrids, the EMS provides accurate information on energy storage as well as demand response (Robert et al., 2018). A building microgrid EMS has been proposed to limit the quantity of power and heat traded with the external system (Bui et al., 2019). The strategy can maximize internal energy trading strategies for optimum hierarchical energy management of integrated cooling, heat, and power. In 2019, a Double Deep Q-Learning-Based distributed management approach for controlling the movement of a residential microgrid battery storage system was developed (Bui et al., 2020), which can cope with system uncertainties in both on-grid and off-grid scenarios. One of the most developing disciplines is load balancing in sustainable EMS for a resilient and reliable power grid (Yang et al., 2019), which includes the active performance of hybrid microgrid energy storage in batteries (Kumar et al., 2020). With the increase in the efficient usage of batteries, battery energy management, and demand-side management has come to the foreground. With the proper development of battery energy management, the stored energy will be used in electric vehicles at a low cost (Tete et al., 2021). In 2021, some researchers proposed an energy loss reduction of the hybrid microgrid system with low-cost battery system

management where a reinforcement learning-based EMS is applied (Rahim et al., 2019). Energy storage technologies include electrochemical and battery energy storage, thermal energy storage, thermochemical energy storage, chemical, and hydrogen energy storage (Shehzad Hassan et al., 2019), and storage energy management is critical to improving the safety, reliability, and cost-effective performance of storage (battery) systems (W. C Li et al., 2020). Using an efficient EMS, the Lead batteries, Li-ion batteries, sodium-sulfur batteries, flow batteries, and supercapacitors are all well-known in the automotive, residential, and industrial markets, and have been successfully used for utility energy storage (Dubarry et al., 2019). In the integrated microgrid, generally, four types of management and operational concern are very much important.

- Power Quality: On a short-term basis, generation, power quality, frequency, and active/reactive power balance must be maintained inside the microgrid.
- Planning: Energy generation, supply, and storage must be carefully designed in relation to microgrid load demand and long-term energy balance.
- Metering and Protection: Microgrid controls should include metering, control, and protection capabilities based on the SCADA.
- Economic Performance: Generation schedules, economic dispatch, and efficient power flow procedures should all be used to guarantee cost-effective operation.

If power quality, proper planning, metering, protection, and economic analysis and control are accurately maintained, then the operation of an integrated microgrid system will benefit in different aspects.

In this research work, a microgrid EMS is developed using linear programming optimization methods. Compared with the traditional heuristic method, the optimization method has less complexity and is easy to operate. This method gives a fast analysis response of controlling and reducing the energy consumption of residential areas or houses or buildings. This method gives accurate control information about the planning and operation of energy generation and various consumption units. Linear programming optimization has been applied to the integrated microgrid (building, residential, university, factory, commercial, etc.) energy management. This EMS performs in a specific selective way, which is set by the operator (Fig. 1). Firstly, it collects and checks the plant's capacity, generation, load demand, forecast cost, etc. information. Then, it evaluates the demand response and analyzes the efficient operation of demand-side management. After analyzing the possible efficient operation, it gives control permission for the final operation. It also monitors every single data of operation and it also re-checks every single step for cost-efficient decision making. The suggested optimum EMS may be implemented using either a single-interval day-ahead economic dispatch model or a multiple-interval day-ahead economic dispatch model for distributed energy resource scheduling. The linear programming technique will be used to initiate, monitor, and regulate solar energy generation, different load projections, and battery energy storage information using the single interval day-ahead mode. This optimization produces a distributed energy resource scheme for each hour the following day, which is then deployed through economic dispatch the following day. The weather variation and the erratic behavior of solar PV systems are monitored and studied using data from an automated meteorological measurement center. This will aid in the control of variable load forecasts and the implementation of effective demand-side management. When the solar system provides less power than demand, the energy storage system will support the different loads, and the grid feed-in mode will activate, allowing energy from the central grid to be injected into the integrated microgrid. In real-time, the day-ahead mode provides cost-effective and efficient energy management.

This research work aims to model and analyze a 10 MW solar PV and battery-based integrated microgrid system. The traditional heuristic method and linear programming optimization method-based EMS have

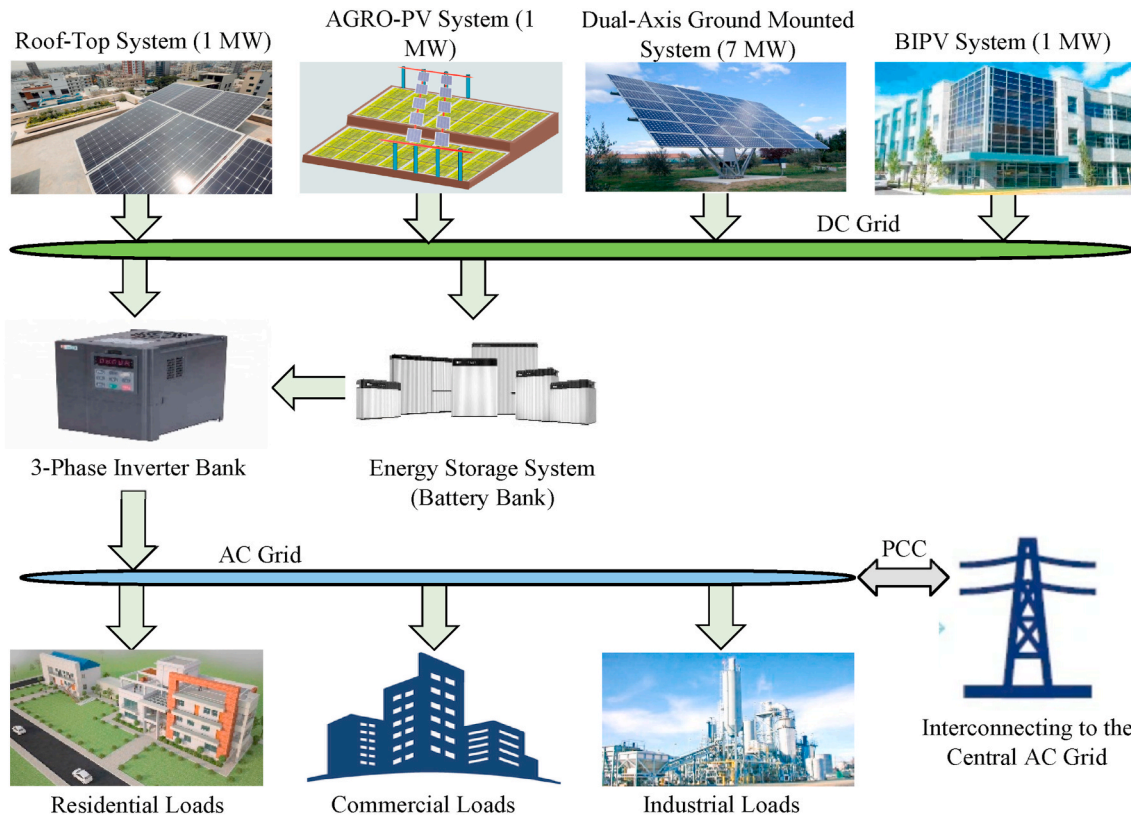


Fig. 2. Suggested solar/battery-based integrated microgrids.

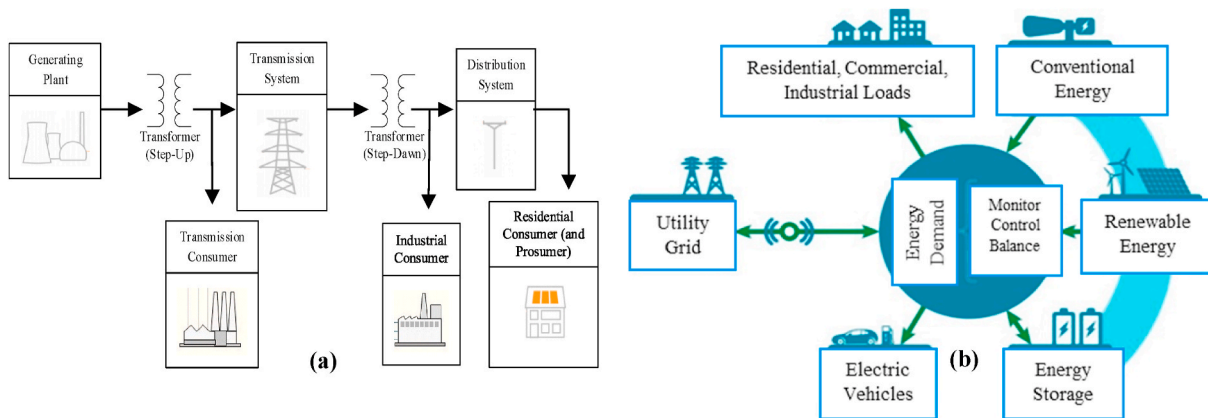


Fig. 3. (a) Power flow diagram of integrated grid system, (b) basic diagram of integrated microgrid EMS.

also been developed to compare their performance in integrated microgrid management. Therefore, a cost-effective EMS is proposed to maintain the energy balance between the solar-based generation and the variable load sides. The main objectives of the proposed linear programming optimization-based EMS are to maximize the output power of solar energy, minimize the operating costs, increase the lifetime of the energy storage system, and ensure uninterrupted power operation and a clean environmental balance. Therefore, the suggested renewable-based integrated microgrid system can be tested with efficient, optimized energy management systems in a real-time environment.

The significant contribution of this research work is the development of a constrained linear program-based optimization approach in renewable energy and battery-based integrated microgrid energy management. To assess the performance of the suggested EMS, a comparison between the proposed optimum linear programming technique and the

conventional heuristic approach is shown. The MATLAB Simulink simulation results proved the cost-effectiveness and better performance of the proposed linear program-based optimization approach by comparing it with the heuristic approach using state flow machine logic/strategy.

The rest of the paper is organized as follows. Section 2 illustrated the description and performance indices in detail of the evaluation of solar PV and battery-based integrated microgrids. Section 3 described the overall methodology, system modeling, control, and operation techniques for performance analysis of integrated microgrid energy management. Following that, the simulation experiments on the microgrid EMS, result analysis, and key findings are discussed in Section 4. Lastly, the conclusions and outlook are presented in Section 5.

## 2. Description and performance indices of integrated microgrid energy management system

Fig. 2 represents the suggested smart integrated grids, where the combination of roof-top PV, Agro-PV, dual-axis ground-mounted PV, and BIPV system makes a smart solar energy hub. In the integrated grid system, the distribution network is connected to the AC bus via circuit breakers, and the AC bus controls the microgrid operation system through the circuit breaker at the point of common coupling (PCC). Different solar-based DGs, and ESSs are connected to the DC bus. Various loads (e.g., residential, commercial, industrial, hospital, educational, agricultural, religious and charitable organizations) are connected to the AC bus (Fig. 3). The integrated grid system is interconnected to the central AC grid via PCC. Because of the intermittency behavior of the solar system, the ESS plays a massive role in feeding power into the integrated AC grid when needed. Therefore, the optimized control of ESS is a very critical and prime concern. Though it is a multi-DG microgrid, several DGs are present, so coordination and control of DGs are pretty complex. Depending on the capacity and demand parameters, the integrated grid will be able to apply as a corporate, feeder area, substation area, or independent microgrid mode. The pre-required mode will be assigned according to different consumer demands by smart EMS's control and monitoring unit.

### 2.1. Various performance indices of integrated solar system

The energy produced by suggested different solar systems  $P_{AC}$ ,  $Y_A$ ,  $Y_R$ ,  $Y_{All}$ ,  $PR_Y$ ,  $\eta_{inverter}$ ,  $P_{PV(total)}$ ,  $CUF$ ,  $\eta_{sys(day)}$  and  $LCOG$  parameters are some of the worldwide performance criteria and standards used in assessing the performance of integrated PV systems. These performance indices describe integrated solar power plant productivity and make it easier to evaluate the characteristics of different solar systems depending on geography and seasonal variations, accessible solar irradiation data monitoring and analysis, grid integration, smart energy-efficient innovation, production of renewables, and cost-effective energy management.

**Geography and Seasonal Variations:** Bangladesh is a country in South Asia, bounded on the east, north, and west by India and on the south by the Bay of Bengal. Due to its location in the foothills of the Himalayas, the climate and temperate is quite noticeable here. As a result, there are six seasons throughout the year, but summer, monsoon, and winter are the three most significant seasons. Naturally, the total solar radiation in summer is more than 11 h per day, while the monsoon and winter seasons have around 8 h per day. Therefore, the suggested system is assumed to have average solar radiation, where the solar power generation duration is around 7 h per day.

**Data Monitoring and Analysis:** The Surface Solar Radiation Database - SARAH, provided by the Photovoltaic Geographical Information System (PVGIS) of the joint research center of the European Commission was used to determine the photovoltaic measurement sites. The PVGIS provides accessible solar radiation data ( $W/m^2$ ) for the USA, Europe, Africa, and Asia and can be accessed via this link (<http://re.jrc.ec.europa.eu/pvgis.html>). Besides, the sun's irradiance, weather conditions, and wind pattern statistics are recorded at a shared automated meteorological measuring center near the integrated microgrid. A central server also uses the SCADA approach to analyze the observed statistics. Generally, on a minute or hourly basis, the server tracks the various solar PV panel data (e.g., current, voltage, efficiency), monitoring sensors data, power quality, inverter performance, other device performance, and inverter through busbar data. It sends the observed data files regularly, and the data is retrieved by the server. In a control booth, the server and SCADA system is kept. From those center, experimental solar radiation data is collected for Raozan (22.5349° N and 91.9104° E) integrated microgrid, Chattogram, Bangladesh. This solar radiation data is tested at STC in the Solar Lab, Institute of Energy Technology,

Chittagong University of Engineering and Technology, Raozan-4349, Chattogram, Bangladesh.

**Solar System Indices:** The STC is determined by the 25 °C ambient temperature and 1  $kw/m^2$  solar irradiation. The solar radiation data provide global irradiance data ( $W/m^2$ ) for a horizontal surface, for an optimal inclined surface, and for a dual-axis sun-tracking surface for daily, monthly and annual averaged. For the analysis, the daily solar irradiance data (clear day and cloudy day radiation data) on an optimally inclined surface is used, as the measuring stations is optimally aligned. Solar panel efficiency is denoted by,

$$\eta_{PV} = \frac{\text{Output electrical energy per second}}{\text{Incided light energy per second}} = \frac{P_{max}}{G \text{ or } P_{in(irra)}} = \frac{I_{SC} \times V_{OC} \times FF}{G \text{ or } P_{in(irra)}} \quad (1)$$

Here, the short circuit current ( $I_{SC}$ ) is calculated when no-voltage is dropped across the circuit. It is depends on solar cell technology, solar cell area and amount of solar radiation in a particular time. The open circuit voltage ( $V_{OC}$ ) is calculated when no-current flows through the solar circuit. It is depends on solar cell technology and solar cell temperature. The Fill factor (FF) is indicate the quality/condition of solar cell. If its FF value is high, solar cell quality is better. The value of FF lies between around 0.8 to 0.9. The avg. global/measured irradiance value for this solar PV cell at STC is,  $G \text{ or } P_{in(irra)} = 1000 \frac{W}{m^2} = 1 \frac{kW}{m^2}$ . Solar PV panel having,  $I_{SC} = 355 \frac{A}{m^2}$ ,  $V_{OC} = 0.74V$ ,  $FF = 0.81$ . So,  $\eta_{PV} = \frac{355 \times 0.74 \times 0.81}{1000} \times 100 = 21.28\%$ . Therefore, the proposed solar PV panel area in this experimental microgrid area ( $A_{PV}$ ) is around 2650  $m^2$ , and the panel array efficiency is = 21.28%.

The time it takes for the PV panel to perform with optimum solar generator power to provide an array's DC energy output ( $E_A$ ) each day is referred to as array yield ( $Y_A$ ). The ratio of the entire in-plane irradiation ( $H_T$ ) and the PV's reference irradiance ( $G$ ) is defined as the reference yield ( $Y_R$ ). It denotes the best possible circumstances for obtaining solar energy. It reflects the amount of peak solar radiation (sun hours) in  $kW h/m^2$  at STC global irradiance. The solar radiation availability for the PV system is also characterized by it at STC. It depends on the location, the PV array's orientation, and weather variations from month to month and year to year (Shiva Kumar and Sudhakar, 2015). The ratio of the system's daily, monthly, or yearly net AC power production and the installed PV array's peak power at STC is referred to as the overall yield ( $Y_{All}$ ). It also approves different solar systems in a given region to be evaluated (Gong et al., 2020). The overall yield and reference yield ratio are referred to as the yield performance ratio ( $PR_Y$ ). The correlation between real and theoretical system performance is described by  $PR_Y$  (C. W Li et al., 2020). It is calculated as the comparison of actual outcomes to the output that the plant might have attained if module technology, size, radiation, panel temperature, temperature adjustment values, mounting system, space area, grid accessibility, and nominal power output are all considered (Tang et al., 2021).

$$Y_A = \frac{E_A}{P_{nominal}} = \frac{V_{DC} \times I_{DC} \times t}{P_{nominal}} \quad (2)$$

$$Y_R = \frac{H_T}{G_{STC}} = \frac{\frac{kWh}{m^2}}{\frac{kW}{m^2}} \quad (3)$$

$$Y_{All} = \frac{E_{PV(AC)}}{P_{G,max(STC)}} = \frac{kWh}{kW_p \text{ day}} \quad (4)$$

$$PR_Y = \frac{Y_{All}}{Y_R} \quad (5)$$

**Integrated Solar System Indices:** The monocrystalline solar panels are used in the dual-axis ground-mounted system (7 MW) and roof-top system (1 MW), besides approximately 20% transparent BIPV (Thin-Film) panels are used in the BIPV system (1 MW) and Agro-PV System (1 MW). Therefore, the total integrated solar system generation capacity is

**Table 1**  
Installation component specification of integrated microgrid system.

Component	Specifications
Solar Block	Total experimental microgrid area ( $A_{PV}$ ) is around 2650 m <sup>2</sup> , where ground-mounted, roof-top, BIPV, and Agro-PV solar systems are around 7, 1, 1, and 1 MW, respectively.
Inverter Bank	About 8 MW three-phase inverter bank is used (Four single-inverter capacities are each 2 MW).
Storage Bank	Structure of simplified battery properties, Energy storage rated capacity, $Batt_{cap(total)} = 2,520$ kWh. Battery Min Discharge Rate, $P_{min} = -400$ kW. Battery Max Charge Rate, $P_{max} = +400$ kW.
Various Load	Around 4,000 kW (including residential, commercial, industrial, hospital, educational, agricultural, religious, and charitable organizations load).

about 10 MW. Their combined efficiency is calculated at around 21.28%. There are different types of loads connected to the smart grid, mainly divided into different types: residential (fixed load), commercial, industrial, hospital, educational, agricultural, and other loads. The daily load curve is analyzed in result part. The forecast grid load or base-load is assumed to be 3,600 kW, and the pick-load is around 400 kW. Therefore, the total load is calculated at around 4,000 kW (See Table 1). The heuristic and linear optimization approaches are applied to the load for efficient energy management. There is a combination of four 2 MW inverters used, which makes an 8 MW three-phase inverter bank. The following equation determines the amount of battery current or DC current ( $I_{DC}$ ) required to fully operate an AC load of 4,000 kW. The ratio of the output AC power provided by the inverter to the input DC power generated by the integrated PV array system is referred to as the inverter efficiency ( $\eta_{inverter}$ ) (Zhang et al., 2021).

$$P_{load} = V_{DC} \times I_{DC} \quad (6)$$

$$\eta_{inverter} = \frac{P_{AC}}{P_{DC}} \quad (7)$$

**Energy Storage System Indices:** Due to its intermittent nature generated solar energy must be stored in strong cascaded battery banks (Lithium-ion). The storage system is very important for proper demand-side management. Suggested integrated microgrids backup storage capacity (days of autonomy) is around one day. About 250 Ah ranged single battery ( $Batt_{size(single)}$ ) bank is used for better performance. Generally, total battery bank size ( $Batt_{size(general)}$ ), Lithium-ion battery size  $Batt_{size(li-ion)}$  and Single battery bank capacity,  $Batt_{cap(single)}$  is determined by (Xie et al., 2021),

$$Batt_{size(general)} = \frac{P_{load} \times t}{V_{DC}} \quad (8)$$

$$Batt_{size(li-ion)} = \frac{100 \times I_{DC} \times t}{100 - Q} \quad (9)$$

$$Batt_{cap(single)} = Batt_{size(single)} \times V_{DC} \quad (10)$$

$$Batt_{cap(total)} = Batt_{cap(single)} \times N_{Batt(single)} \quad (11)$$

In a single li-ion battery,  $V_{DC}$  is selected as 48 V, then  $Batt_{cap(single)}$  is calculated as 12 kWh. The number of single battery banks,  $N_{Batt(single)}$ , is measured as 210 times the capacity of  $Batt_{cap(single)}$  to create the total battery bank capacity,  $Batt_{cap(total)}$ . Therefore,  $Batt_{cap(total)}$  is calculated as around 2,520 kWh. Generally, the daily load profile of the battery bank is utilized by the autonomy (backup time) method, which is also known as the battery bank characteristics. Those different characteristics are given by the datasheet of the manufacturer, which are temperature, ampere-hour capacities, float voltage, total charge li-ion electrolyte density, and cell end-of-discharge voltage type battery bank data. The number of battery banks necessary can be determined with greater precision to better match the load tolerance (Jordehi et al., 2020a). The

ratio of battery banks planned to be connected in series or parallel should lie between the following two limits:

$$N_{Batt(max)} = \frac{V_{DC}(1 - V_{load(max)})}{V_{DC}} \quad (12)$$

$$N_{Batt(min)} = \frac{V_{DC}(1 - V_{load(min)})}{V_{eodv}} \quad (13)$$

To accommodate the load over the defined autonomy, a minimum charging capacity in ampere-hour (Ah) of the battery bank is necessary (Cao et al., 2021). The amount of uninterrupted DC current required to charge the 2,520-kWh battery bank is defined as the battery bank charging current. At the same time, the amount of DC current required in the solar panel to adequately run the load and charge the battery is defined as the solar panel's total current ( $I_{PV(total)}$ ).

$$C_{Batt(min)} = \frac{E_{DC}(k_{af} \times k_{icf} \times k_{crt})}{(V_{DC} \times k_{mdod} \times k_{sc})} \quad (14)$$

$$I_{Batt, char(DC)} = \frac{1}{10}^{th} \text{ of } Batt_{cap(total)} \quad (15)$$

$$I_{PV(total)} = I_{DC} \times I_{Batt, char(DC)} \quad (16)$$

Total solar system power ( $P_{PV(total)}$ ) or installed capacity of the plant identified by,

$$P_{PV(total)} = V_{DC} \times I_{PV(total)} \quad (17)$$

**Other Indices of Integrated Solar System:** The capacity utilization factor (CUF) is the difference between the plant's actual output energy and its potential maximum output energy if it will run at full strength 24 h a day or 365 days a year (Bansal et al., 2021). The CUF is determined by incident irradiance, weather, the number of clear bright days, the number of gloomy wet days, grid integration, and energy storage technology used (Allouhi et al., 2019). The LCOE is directly affected by CUF.

$$CUF = \frac{E_{PV(AC)}}{365 \times 24 \times P_{PV(total)}} = \frac{Y_{All}}{365 \times 24} \quad (18)$$

The daily PV module efficiency multiplied by the daily inverter efficiency represents the daily solar PV system efficiency ( $\eta_{sys(day)}$ ). It also indicates the ratio of the energy fed into the integrated grid to the irradiation accessible across the whole solar PV system area (Daneshvar et al., 2020). Internal PV cell efficiency, inverter and transformer performance, wire losses, system unreliability, and other factors all have an impact on it (Gazijahani et al., 2020).

$$\eta_{sys(day)} = \eta_{PV(day)} \times \eta_{inverter(day)} = \frac{E_{PV(AC)}}{A_{PV} \times P_{in(irra)}} = \frac{E_{PV(AC)}}{A_{PV} \times G} \quad (19)$$

The price of one unit of energy supplied in USD/kWh is known as the LCOE. It is a metric for comparing the cost-effectiveness of several power generation systems. It is calculated by dividing the entire cost of establishing, administering, and servicing the PV system by the total electricity produced throughout the project's lifetime (Sedighzadeh et al., 2020). The yearly O & M expenses encompass the annual monitoring, maintenance, repair, replacement, labor costs, and renewal prices of different types of equipment, such as proposed PV modules, mechanical supports, connecting cables, bypass diodes, three phase inverters banks, battery banks, protectors, etc. costs.

$$LCOE = \frac{\sum_{t=1}^n \left\{ \frac{I_t + (O\&M)_t}{(1+r)_t} \right\}}{\sum_{t=1}^n \left\{ \frac{E_t}{(1+r)_t} \right\}} \quad (20)$$

Evaluating deterioration processes and fault detection involved with PV panels in their surroundings is critical for ensuring the long-term dependability of solar PV systems (Chen et al., 2020). The yearly energy degradation rate is affected by a variety of factors, including

**Table 2**  
Difference between heuristic method and optimum linear programming method.

Heuristics method	Optimum linear programming method
A heuristic strategy is a problem-solving strategy that employs a practical strategy in limited timeframe.	Optimization is the process of finding the minimal or greatest value of a function by choosing variables, subject to constraints.
Heuristic methods achieve an immediate goal but not necessarily an optimal solution.	The challenge of supply chain scheduling and planning lies at the heart of an optimization strategy.
These methods are unable to implement an optimal solution (Mansouri et al., 2021).	There are several linear programming techniques to solving optimization issues.
Main advantages of using a heuristic method are that it provides a rapid solution/answer that is simple to understand and implement.	The primary benefit of optimization approaches is that they deliver the best feasible solution to a given planning and scheduling problem (Yassuda Yamashita et al., 2021).
Better output in a short length of time, that makes real-time operational settings easier.	Optimization is a natural choice since solution quality is typically a significant success element for tactical and strategic supply chain optimization decisions (De et al., 2021).

obtainable direct solar radiation, weather conditions, moisture levels, implemented PV technology, PV producer, PV module alignment, soiling, mechanical support, the direction of wind patterns, systematic errors, measured failure modes, methodological approach, analytical operation, and so on (Moazeni and Khazaei, 2020). The integrated solar system's yearly deterioration is determined by the classical decomposition/linear regression (regression coefficients such as  $a_{slope}$  and  $b_{intercept\ of\ linear\ trend}$ ) statistical method or the maximum energy observed method (Cortés et al., 2020).

$$Degradation_{year} = 100 \times \left\{ \frac{12 \times a_{slope}}{b_{intercept\ of\ linear\ trend}} \right\} = \frac{100 \times (P_{nominal} - P_{present})}{P_{nominal} \times Age\ of\ operation} \quad (21)$$

Generally, the power produced by the PV system is monitored throughout the three-phase inverter output endpoints every minute, which is recorded and analyzed for energy management. Those experimental data sets are essential for energy efficiency analysis. It is specified as the total hourly or daily recorded AC power output, giving the monthly AC power generation, distribution, and utilization analysis.

### 2.2. Optimal process and measurements of integrated solar system

Several pre-required optimization factors must be addressed to attain the appropriate sizes and numbers of each power-generating integrated unit. HOMER provides an optimal COE and NPC for a solar-based integrated system. These metrics provide an accurate economic assessment of the microgrid's operation (Aghdam et al., 2020). The combined electricity produced by each resource must be larger than or equal to the integrated microgrid's maximum demand, various losses and energy storage (Naik et al., 2021).

$$\frac{\min}{a, b, c, d, f_1 \in N^{\circ}} (f_1(a, LCOE_{RTPV} + b, LCOE_{APV} + c, LCOE_{GMPV} + d, LCOE_{BIPV} + e, LCOE_{Batt})) \quad (22)$$

$$\frac{\min}{a, b, c, d, f_2 \in N^{\circ}} (f_2(a, NPC_{RTPV} + b, NPC_{APV} + c, NPC_{GMPV} + d, NPC_{BIPV} + e, NPC_{Batt})) \quad (23)$$

$$\frac{\min}{emis, f_3 \in N^{\circ}} (f_3(emis, GHG_{microgrid})) \quad (24)$$

$$\frac{\min}{f_1, f_2, f_3 \in N^{\circ}} (f_1 LCOE_{Total} + f_2 NPC_{Total} + f_3 GHG_{Total}) \quad (25)$$

$$COE = \frac{C_{total,year}}{P_{total\ load} + P_{total\ def} + E_{grid,sales}} \quad (26)$$

$$NPC = \frac{C_{total,year}}{C_{RF}(i, L_{microgrid})} \quad (27)$$

$$P_{total\ max\ power\ generation} > P_{total\ load} + P_{loss} + P_{Batt} \quad (28)$$

The economic dispatch schedule provides the output price of all available solar generating units in the power system for better optimization. All generated electricity must be equivalent to the electricity demand in order for the solar system to retain its maximum and lowest limits (Dey et al., 2021).

$$P_{PVG,i}^{min} \sum_i C_{PVG,i} P_{PVG,i} \quad (29)$$

Where,  $P_{PVG,i}^{min} \leq P_{PVG,i} \leq P_{PVG,i}^{max}$  and  $\sum_i P_{PVG,i} = P_{total\ load}$

### 2.3. Energy management system of integrated microgrid

**Distributed Energy Resources (DER):** Microgrid (heterogenous energy resources) equipped with energy storage methods presents the idea of DER management. It simplifies the reduction of the generation, transmission, distribution, operation costs, peak load, and environmental pollution. By offering customers access to real-time information and control, the EMS enables active consumer engagement. It also provides the capacity to quickly recover from physical or cyber-attacks (Kermani et al., 2021). Microgrids are an attractive alternative for distributed power systems because they integrate renewable energy resources and information and communication technology (ICT) (Kumar et al., 2021). The DER are power generation units situated within the electrical distribution system area or near the end-user (Jordehi et al., 2020b).

The control methods of DER are distinguished in a proposed inte-

grated microgrid by their interface characteristics (input and output behavior) in real-time observation. The generation control system is divided into rotary DG units and electronic-coupled DER units. Initially, different solar systems are connected to the electronic-coupled DER units of the microgrid. The electronically-coupled DER units use power electronics converters and three-phase inverters to match their various features, power production patterns, and energy storage conditions. The control system for DER units is built within the integrated microgrid management based on the needed functions and likely operational

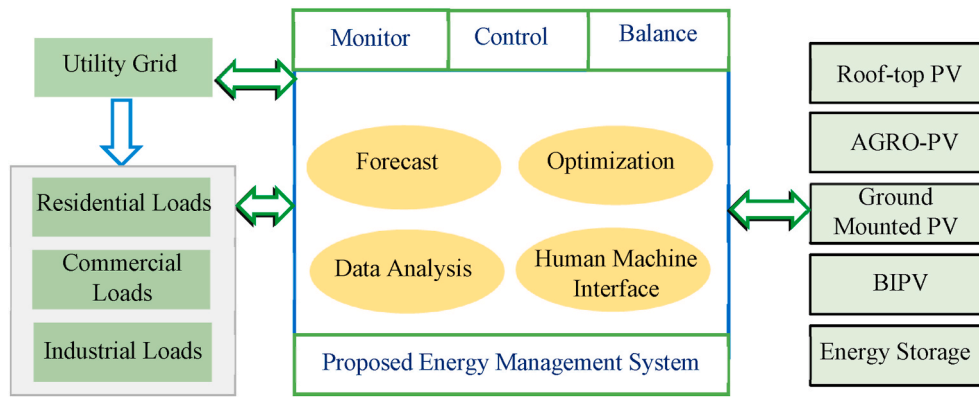


Fig. 4. Working flow of proposed microgrid energy management system.

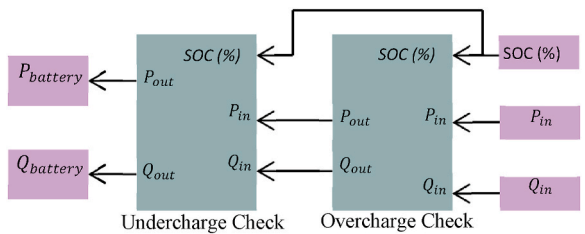


Fig. 5. Flowchart of SoC and DoD for battery storage management.

circumstances. The DER units of the suggested integrated microgrid can operate as a grid-forming unit, grid-feeding unit, or grid-supporting unit mode when necessary. When the microgrid is in island mode, a grid-feeding unit regulates system voltage and frequency by balancing generation power and load needs. The grid-feeding unit is active when adjusting the output active and reactive power based on power dispatch techniques or the feeder frequency and voltage fluctuations of the load. Besides, the grid-supporting unit is available when it is controlled to extract maximum active power and appropriate reactive power from its primary energy source to support grid voltage sags and local reactive current demands.

**Selection of Optimization Techniques for Energy Management System (EMS):** It includes modules for human machine interfaces (HMI), control, and data collecting, among other things, so that it controls automated energy demand-response system and overall system optimization over individual optimization (like energy saving, reduction of CO<sub>2</sub> emission, cost reduction, etc.) (Lee et al., 2016). Minimizing the cost of the system and reducing its negative impacts require optimizing the size of the microgrid components and implementing an efficient EMS. The EMS is primarily integrated with optimization to assure load supply continuity and to decrease the cost of energy generation, production to distribution costs (Mosa and Ali, 2021). As a result, the EMS is a strategy that analyzes all of the systematic procedures for controlling and reducing the amount and cost of energy utilized to meet the needs of a certain application. The EMS is mostly determined by the type of

energy system and the components that make it up. To build an effective EMS, various optimization techniques have been applied, where near-optimal design variables based on non-conventional techniques (e.g., heuristics, meta-heuristics, genetic algorithms) and optimal design variables based on conventional techniques (e.g., iterative mathematical programming, linear, non-linear, and dynamic programming) are most of them (Ahmadi and Rezaei, 2020). Iterative mathematical optimization, often known as mathematical programming, is a sophisticated analytical methodology for solving complicated microgrid problems and making better use of given resources and data. Both linear programming optimization and heuristic solutions aim to find the optimal answer, but their outcomes are often dramatically different. Some benefits and drawbacks of them are attached in Table 2. According to empirical data, linear programming optimization techniques are far superior to heuristic methods (See Fig. 4). Linear programming optimization techniques have quick optimization tools and techniques for integrated microgrids, such as data analysis, data processing, simulation, control, decision making, and optimum management models for hybrid systems of energy generation. Those strategies aid in justifying the expense of a microgrid investment by allowing for cost-effective and predictable resource consumption.

2.4. Control of SoC and DoD for Battery Storage Management

The SoC of an electric battery is the amount of charge it has in relation to its capacity. It is measured in percentage points (0 percent equals empty, 100 percent equals full). Besides, the DoD is a different way of measuring the same thing (SoC). The DoD is exactly opposite of SoC (100 percent equals empty and 0 percent equals full). The SoC is most important and commonly seen in this integrated microgrid system when discussing the lifetime of a battery after repeated usage, whereas DoD is most typically seen while discussing the current status of a battery in operation (See Fig. 5).

3. Methodology and modeling for performance analysis

The recommended solar/battery-based integrated microgrid

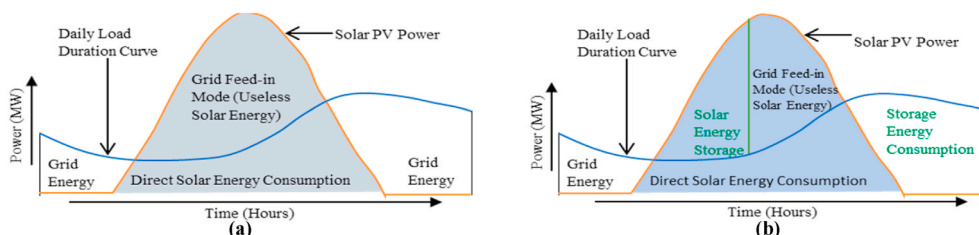


Fig. 6. (A) Daily load duration curve without solar energy storage, (b) peak demand shift using energy storage in traditional EMS.



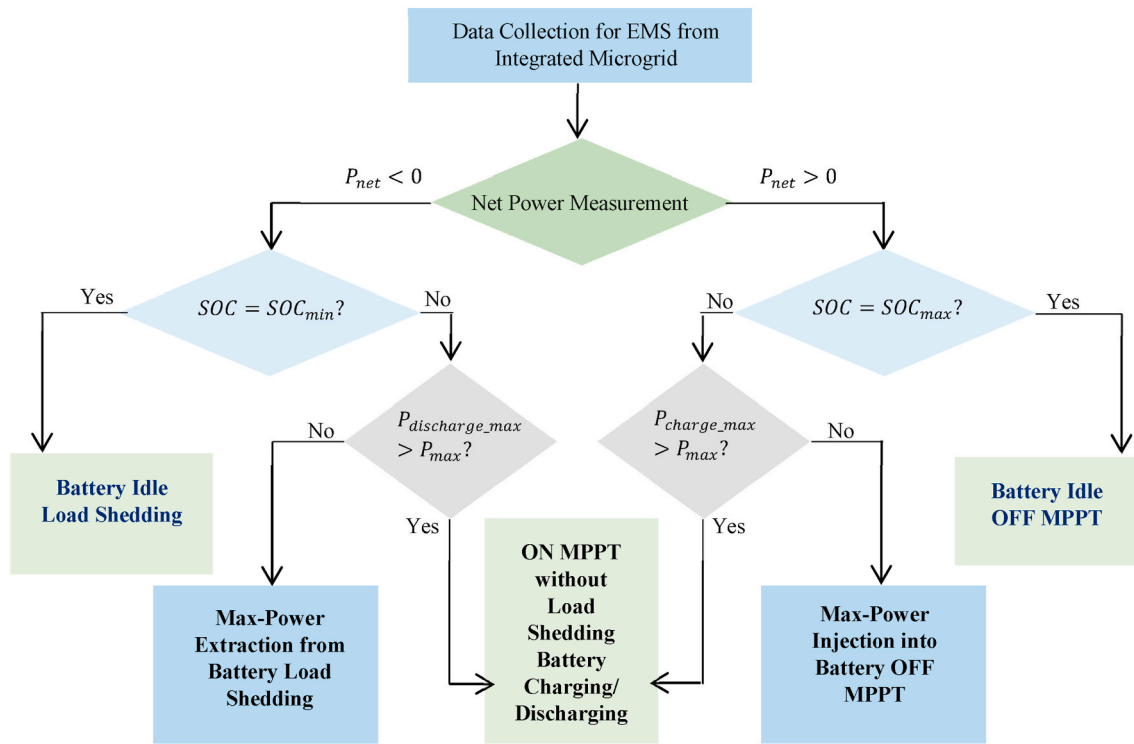


Fig. 7. Microgrid control flowchart of linear optimization EMS.

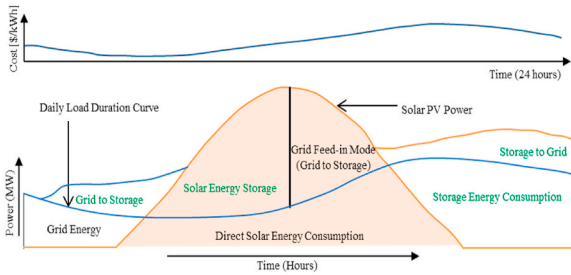


Fig. 8. Peak demand shift using energy storage and factoring in variable electricity cost.

modeling is illustrated in Fig. 2 based on the installation component specifications of Table 1. One whole day is chosen to collect and analyze different critical data for three seasons (summer, monsoon, and winter). Summer is characterized by long, bright days with average solar radiation of more than 11 h each day. Furthermore, owing to occasional rains during the monsoon season, certain variations in the sunshine may be seen. As a result, solar radiation is measured for about 7 h every day. On the other hand, winter has about the same amount of solar radiation as a cloudy day, with roughly 7 h of solar radiation due to the cold temperature. As a result, this experiment counted both the monsoon and winter seasons as the same kind of season and the same solar radiated day. The solar PV system only creates electricity when the sun shines throughout the day. Produced solar energy is immediately injected into the grid in an integrated microgrid system. Compared to evening and nighttime demand, daytime load demand is exceptionally modest. As a result, excess solar electricity must be stored to meet peak load demands. As a result, advanced EMS is necessary for quick load demand-side response. A significant percentage of excess energy is wasted when a renewable energy storage system is not accessible in an integrated microgrid due to inefficient energy management. However, effective microgrid EMS provides the highest results and renewable energy savings. This section discusses the advantages of successful EMS.

*Peak demand without solar energy storage (without EMS):* Renewable energy (solar, wind) systems are directly linked to the grid in a conventional grid system. Due to the lack of energy storage technology, a large quantity of surplus renewable energy is squandered, as seen in Fig. 6(a). When the sun is available, the solar PV system provides electricity, and when it is not, the integrated microgrid may collect the required energy from the central grid as a grid feed-in system.

*Peak demands with battery-connected solar energy storage (traditional heuristic EMS):* The solar PV system is linked to the integrated grid through energy storage (battery) device. The load power profile is relatively low throughout the day; thus, peak demand is shifted or altered, but some surplus solar energy is available in grid feed-in mode (See Fig. 6(b)). Consequently, surplus solar power is not efficiently used in this classic heuristic EMS, and a certain quantity of solar power is squandered. This EMS uses the stored solar energy during solar pick-up hours.

*Linear optimization EMS (Factoring in variable electricity cost):* There are two-step-based coordination controls used to maintain microgrid EMS stable operation. Initially, in this control logic, various operation modes of the solar power generators are determined by the EMS based on the system net power ( $P_{net}$ ) measurement and the charging/discharging rate of the battery system with the energy constraints. The microgrid control flowchart of linear optimization EMS system is shown below in Fig. 7, where net power ( $P_{net}$ ) is calculated from eq. (30). In control logic, the energy constraints of the battery are calculated from eq. (31) based on the SoC limits (Wang et al., 2021). It should be noted that SoC cannot be measured directly, but can be attained through SOC estimation and monitoring methods (Fathima and Palanisamy, 2015). Then, the constraint of charging and discharging rate is determined from eq. (32).

$$P_{net} = P_{total \ max \ power \ generation} - P_{total \ load} - P_{loss} \quad (30)$$

$$SOC_{min} < SOC \leq SOC_{max} \quad (31)$$

$$P_{batt} \leq P_{batt(max)} \quad (32)$$

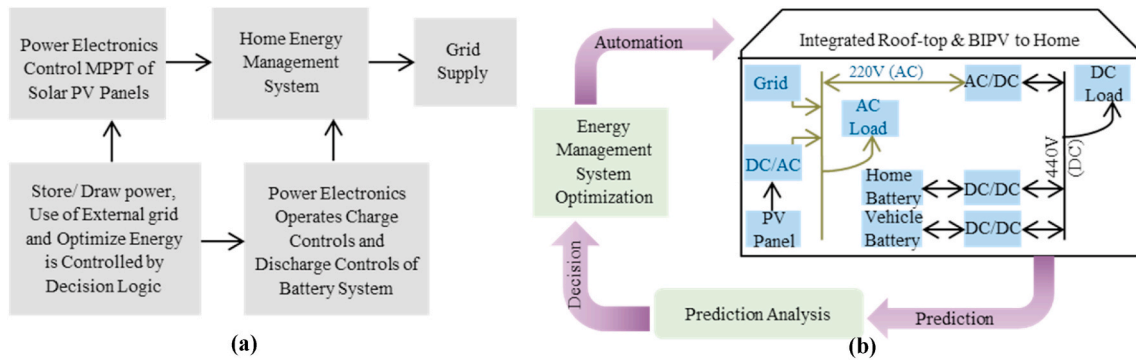


Fig. 9. (A) Working process of smart home energy management system, (b) development of smart home energy management system.

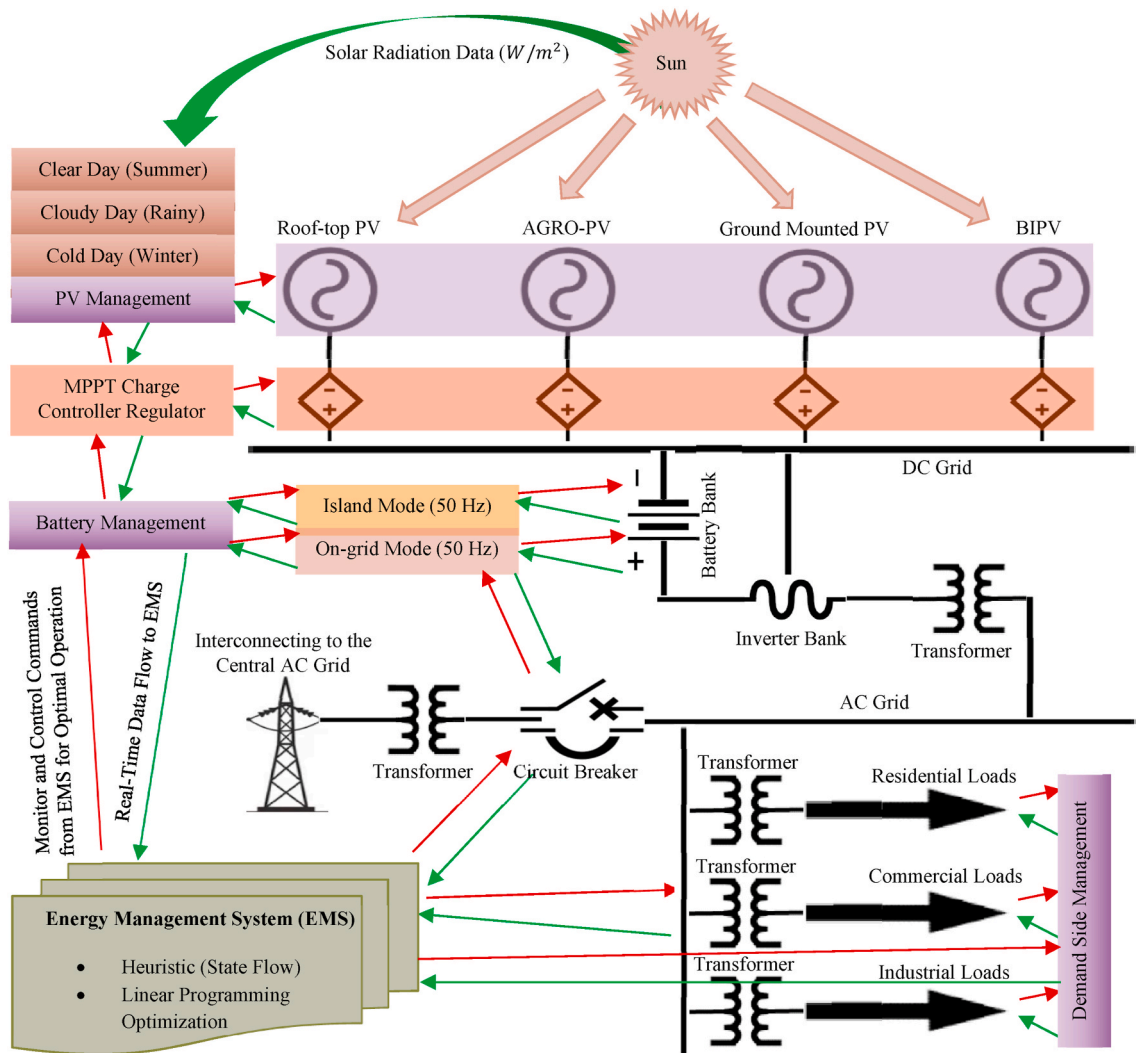


Fig. 10. Test model of microgrid energy management system.

When SoC is in maximum ( $SoC = \text{maximum SoC}$ ) storage condition, the individual solar PV power generator operates based on mode commands from the EMS. At that level, either the ground-mounted solar PV generator or the roof-top solar generator must operate in the off-MPPT mode or the on-MPPT mode for other options. The energy storage system (battery) may operate in the idle, charging, or discharging mode for the different time situation of the linear optimization method. The linear optimization method will operate the battery (storage) to the grid if  $P_{net} - P_{load}$  is negative or the solar to storage/grid to the storage if  $P_{net} -$

$P_{load}$  is positive. If the power supply is less than demand and the battery is at the minimum SoC then load shedding is required to maintain power balance. Comparing Fig. 8 with Fig. 6, the peak demand is shifted, and the grid replaces surplus solar energy grid feed-in mode with a storage grid feed-in mode. This happens during the surplus condition of solar power generation because when the battery is not fully charged, the battery will consume a charge from solar PV and the grid as well. When the battery is fully charged and solar power is not available, at that time the grid is used for the battery power. This process battery is operated in

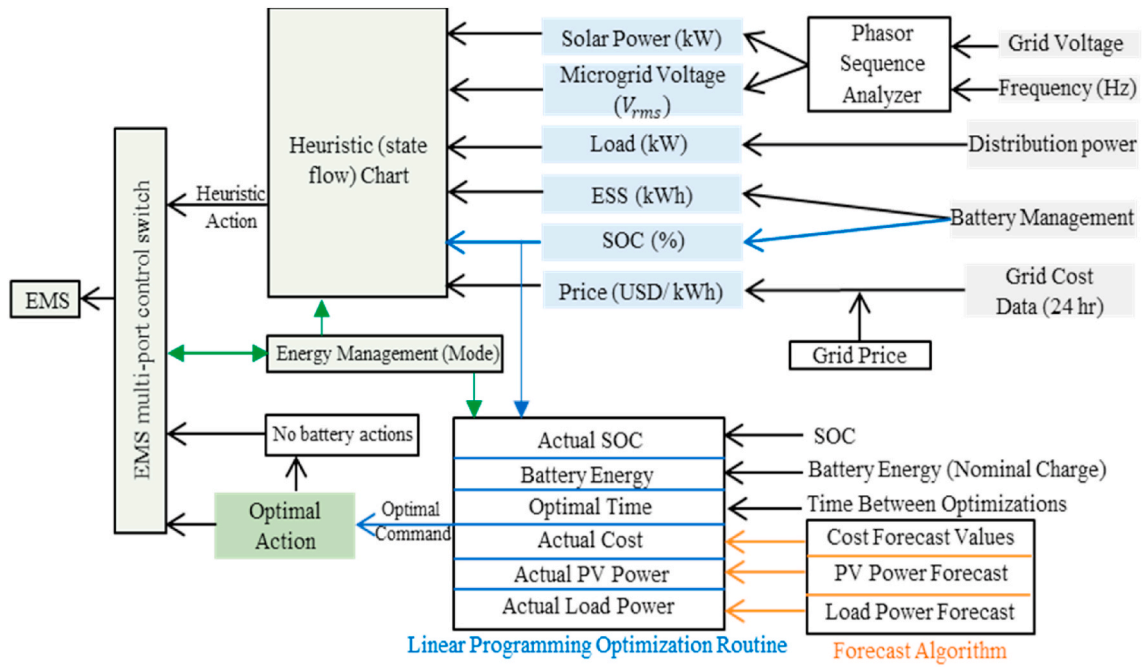


Fig. 11. Working flow of proposed microgrid energy management system.

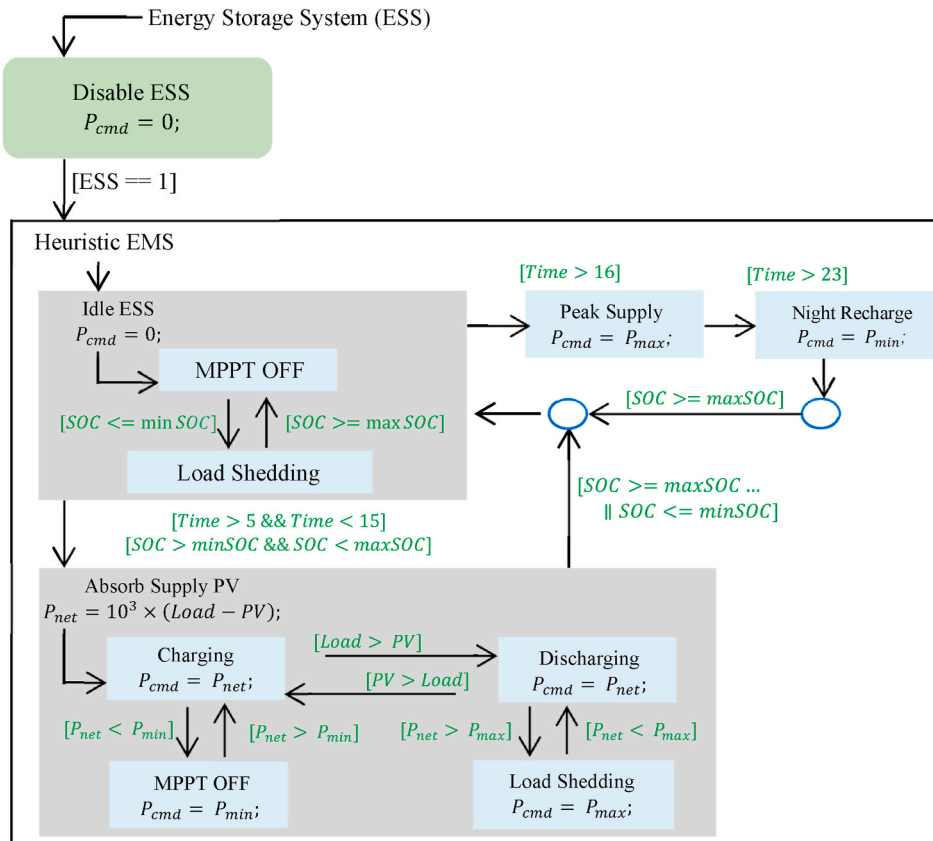


Fig. 12. State flowchart of traditional heuristic method.

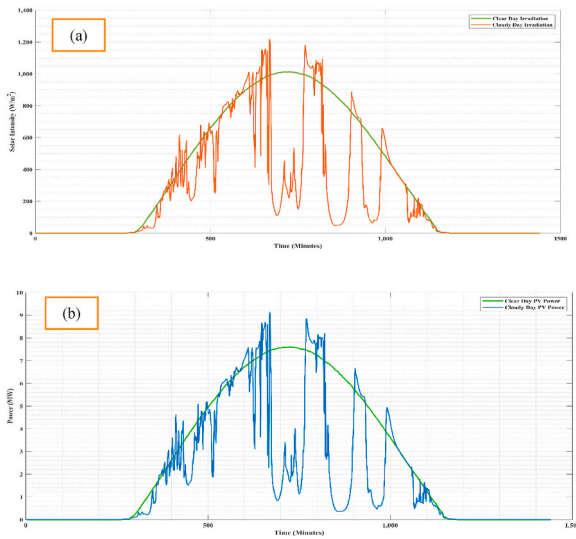


Fig. 13. Measurement of clear and cloudy day (a) solar radiation data, and (b) solar PV array power production.

grid feed-in mode. Furthermore, that is why the total peak demand from the microgrid is reduced because the battery is supplying the power. Therefore, the total cost is minimized by using the optimization EMS. Proposed linear programming optimization EMS will constantly observe demand, and they will give a response to that demand to automatically perform the overall system optimization. Therefore, the whole system's operating cost is significantly reduced.

### 3.1. Residential or home energy management system for roof-top and BIPV solar

The proposed EMS is efficient for residential or home appliances. Home EMS is connected to a microgrid with loads. Fig. 9(a) illustrates the working process of the smart home EMS. Besides, Fig. 9(b) shows the development of smart home EMS, where the home microgrid contains various household power electronic systems. These are almost always present in every house. Here, the optimal linear EMS is operating step by step. First, with the help of a linear optimization algorithm, the prediction process is completed, and the prediction analysis sends the

forecast data to EMS optimization. Then it takes the forecast data. The EMS optimization is performed using the system's constraints from prediction analysis. Finally, the EMS gives an automatic optimal way to use all of those together.

### 3.2. Optimization-based peak demand shift system

The demand-side management is necessary to control and shift the peak load. An optimization-based peak demand shift system applies the optimum linear programming EMS to peak power balance. The objective and constraint functions are performed separately for data analysis and suitable decision-making. The objective function minimizes the total cost of variable-priced electricity from eq. (33). Besides, the total system is operated by power input/output for battery control and power balance optimized management. So, the constraint's function controls the load demand input/output to the battery and power balance of the integrated microgrid. The power input/output to the battery,  $E_{batt}(k)$  and power balance,  $P_{load}(k)$  optimization is calculated from eqs. (34) and (35) respectively. Where, different power generating sources are  $P_{pv}(k)$ ,  $P_{grid}(k)$  and  $P_{batt}(k)$ . And power consuming loads are  $P_{load}(k)$ .  $P_{grid}(k)$  is the optimal vector of grid power (kW) usage,  $P_{batt}(k)$  is the optimized battery (kW) usage, and  $E_{batt}(k)$  is the total battery energy over optimization horizon (Joule).

$$C_{tot} = \sum_{k=0}^N C_{grid}(k) \times E_{grid}(k) \tag{33}$$

$$E_{batt}(k) = E_{batt}(k - 1) + P_{batt}(k) \times \Delta T \tag{34}$$

$$P_{load}(k) = P_{pv}(k) + P_{grid}(k) + P_{batt}(k) \tag{35}$$

### 3.3. Formulation of linear program-based optimization

The cost-effective operation of the suggested solar PV/battery-based integrated microgrid is dependent on precise linear function assignment and modeling, as well as training them for successful real-time operation. The standard form of the linear program (LP) optimization function (*linprog*) is analyzed by eq (36). The selection of various state (x) functions is necessary for absolute time generation control, battery energy management, pick load shifting, and load response. eq (37) computes the state (x) function. The equivalent constraint for LP optimization operations is measured by three different bus matrices such as  $X$ ,  $\gamma_{3 \times 3}$

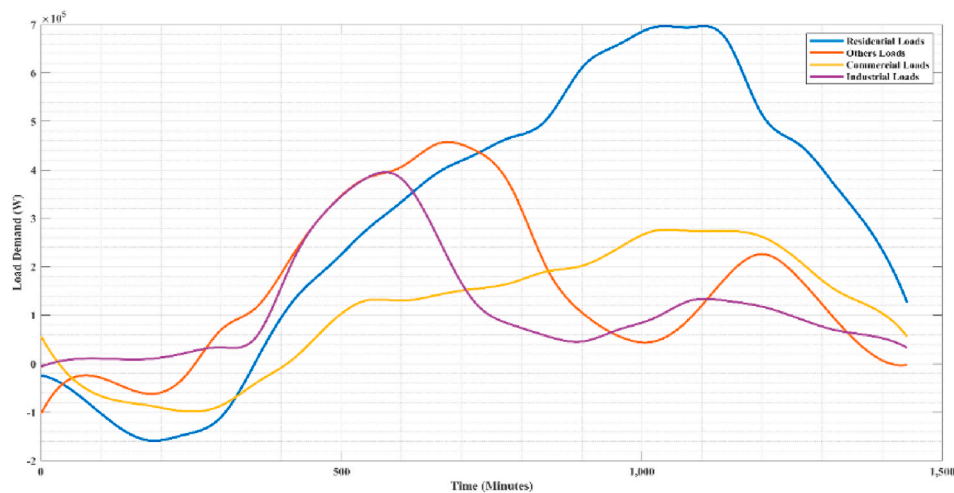


Fig. 14. Load duration curve.

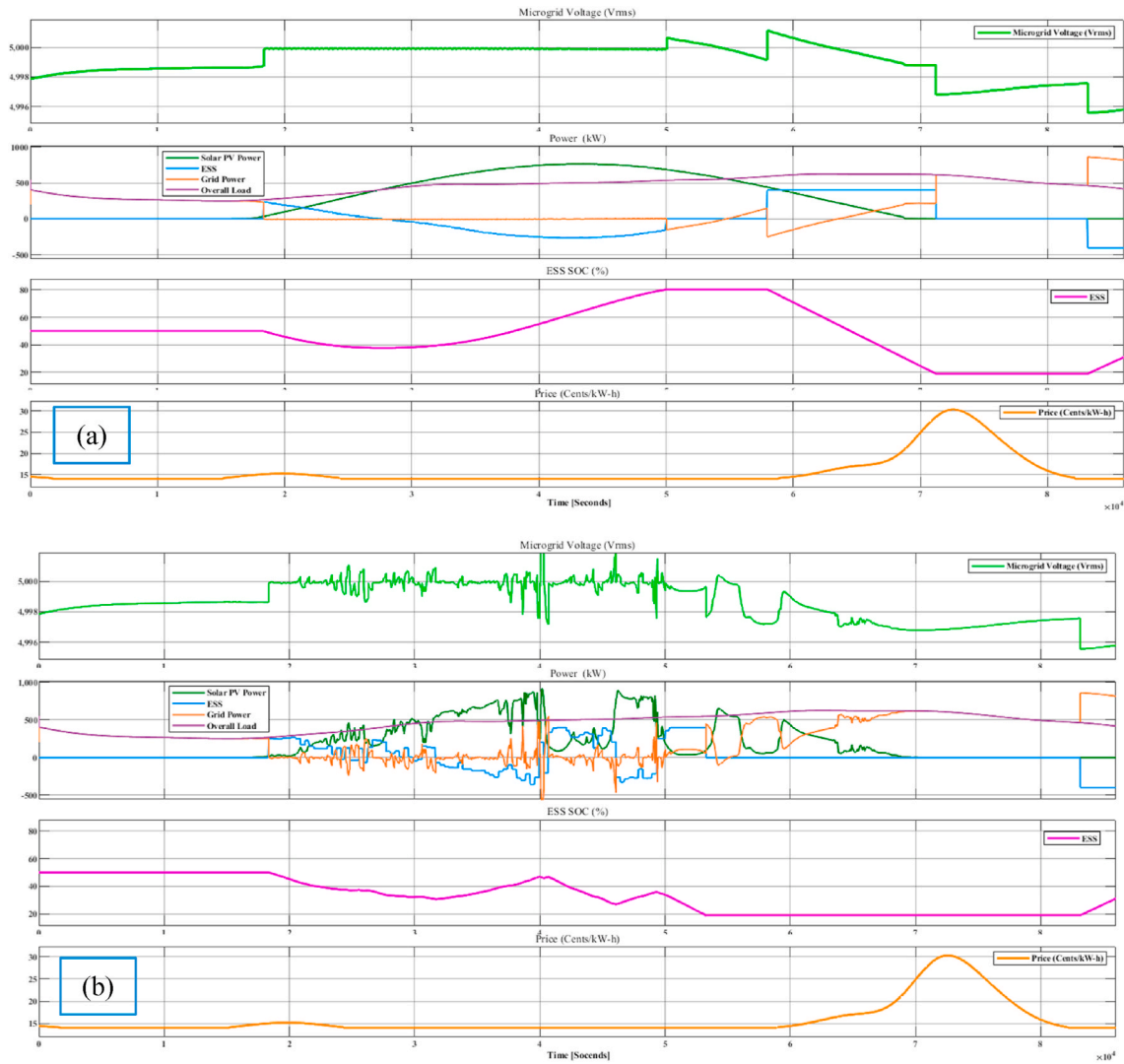


Fig. 15. Various parameter measurements of integrated microgrid on heuristic EMS: (a) Clear day, and (b) cloudy day.

$$\begin{matrix} \downarrow A_{eq} \\ \begin{bmatrix} I_{N \times N} & I_{N \times N} & O_{N \times N} \\ O_{N \times N} & Y_{N \times N} & Q_{N \times N} \end{bmatrix} \end{matrix} X = \begin{matrix} \downarrow b_{eq} \\ \begin{bmatrix} P_{load}(1:N) - P_{pv}(1:N) \\ E_{batt}(1) \\ O_{N-1} \end{bmatrix} \end{matrix} \quad (38)$$

and  $\emptyset_{3 \times 3}$  in eqs (38)–(40) respectively, where  $A_{eq}$  and  $b_{eq}$  are equivalent matrix parameters that control the solar PV system, load, and battery optimization. Besides, the inequality constraints for LP optimization operation are calculated by the inequality bus matrix eq (41), where  $A$  and  $B$  are equivalent matrix parameters that control the maximum/minimum power production ratio of the solar PV system and the maximum/minimum electricity consumption ratio of various loads.

$$\min_x f^T x, \text{ Such that } \begin{cases} A \cdot x \leq b \\ A_{eq} \cdot x = b_{eq} \end{cases} \quad (36)$$

$$\begin{matrix} \downarrow A \\ \begin{bmatrix} O_{N \times N} & I_{N \times N} & O_{N \times N} \\ O_{N \times N} & -I_{N \times N} & O_{N \times N} \\ O_{N \times N} & O_{N \times N} & I_{N \times N} \\ O_{N \times N} & O_{N \times N} & -I_{N \times N} \end{bmatrix} \end{matrix} X \geq \begin{matrix} \downarrow b \\ \begin{bmatrix} P_{max} \\ -P_{min} \\ E_{max} \\ -E_{min} \end{bmatrix} \end{matrix} \quad (41)$$

$$x = [P_{grid}(1:N) \times P_{batt}(1:N) \times E_{batt}(1:N)] \quad (37)$$

Where different states (x) parameters for the LP optimization operation are:

- $P_{grid}(1:N)$  = Power from electric grid used from time step 1 to N.
- $P_{batt}(1:N)$  = Power from battery.
- $E_{batt}(1:N)$  = Energy stored in battery.

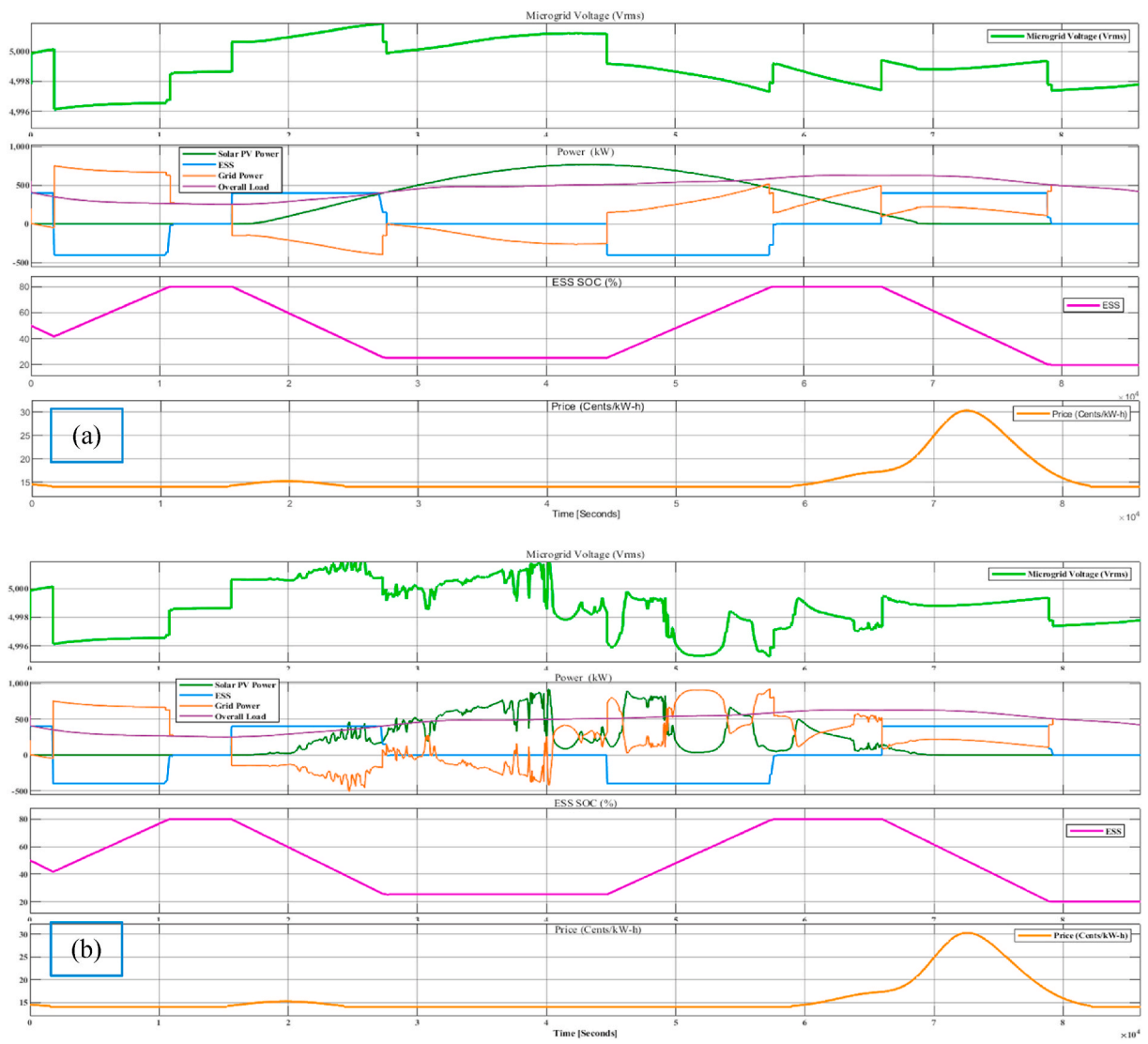


Fig. 16. Various parameter measurements of integrated microgrid on optimal LP EMS: (a) Clear day, and (b) cloudy day.

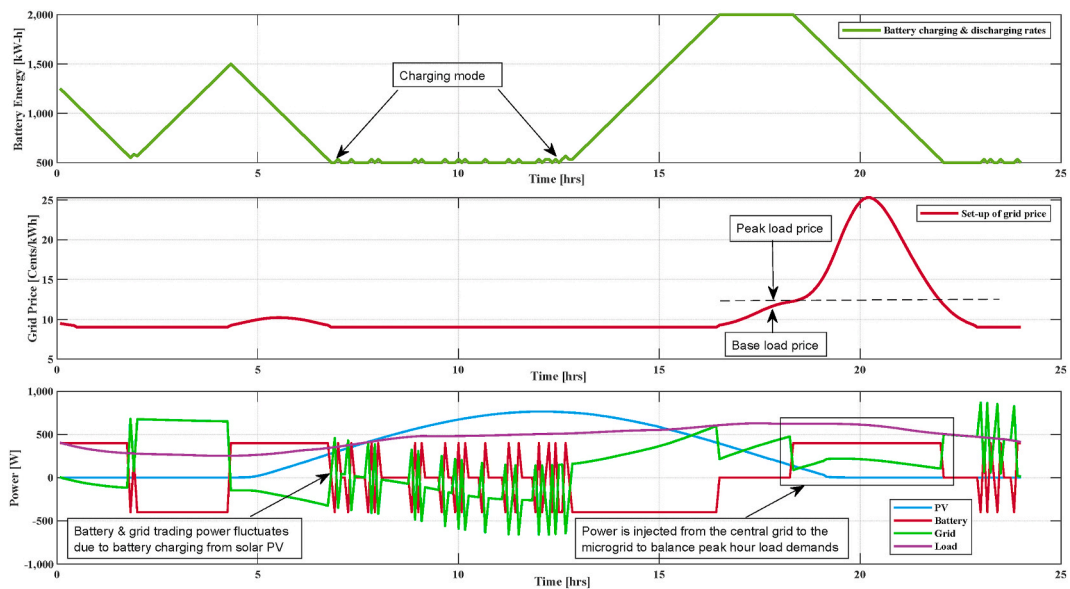


Fig. 17. Set-up of Optimization Parameters of Linear Programming based EMS for Integrated Microgrid.

**Table 3**  
Electricity price for the various consumer categories of integrated microgrid system.

Consumer sector and categories	Demand type and range	Monthly Electricity Price Range \$/kWh	
		Specification: Transmission line (low pressure): 230/400 V Electricity supply: AC single phase 230 V and three phase 400 V Frequency: 50 Hz Load: single phase single 0–7.5 kW and three 0–100 kW	Specification: Transmission line (medium pressure): 11 kV Electricity supply: AC three phase 11 kV Frequency: 50 Hz Load: 101 kW–500 kW
Residential (e.g., Private houses, Apartments)	0-400 kWh	0.13	–
	401-600 kWh	0.15	–
	More than 600 kWh	0.16	–
	Flat hours	0.16	0.17
	Off-peak hours	0.15	0.16
Commercial and Office (e.g., Productive, Non-Productive)	Peak hours	0.18	0.22
	Flat hours	0.18	0.26
	Off-peak hours	0.16	0.22
	Peak hours	0.22	0.30
Industrial (e.g., Productive, Non-Productive)	Flat hours	0.18	0.26
	Off-peak hours	0.16	0.22
	Peak hours	0.22	0.30
Others (e.g., Educational, religious and charitable organizations, hospital and Agriculture)	Flat, off-peak and peak hours	0.12	0.16

Equivalent constraints for LP optimization operation.

$$\gamma_{3 \times 3} = \begin{bmatrix} 0 & 0 & 0 \\ \Delta T & 0 & 0 \\ 0 & \Delta T & 0 \end{bmatrix} \quad (39)$$

$$\emptyset_{3 \times 3} = \begin{bmatrix} 1 & 0 & 0 \\ -1 & 1 & 0 \\ 0 & -1 & 1 \end{bmatrix} \quad (40)$$

Inequality constraints for LP optimization operation.

### 3.4. Modeling and analysis of integrated microgrid EMS

The proposed integrated microgrid is comprised of a utility point of connection, various fixed, static, or primary loads (such as residential, commercial, and industrial loads), various solar PV generation systems (whose input can be used in various radiant modes such as the clear day or cloudy day), inverters, and energy storage systems. The overall test model of the EMS is represented in Fig. 10, which is simulated using the MATLAB Simulink power systems toolbox. The ESS takes input data from the EMS optimization commands and then takes necessary action for generation and load balancing in either grid-connected or off-grid mode operation. The ESS plays a prime role in controlling demand-side management. In this proposed test model, two types of EMS are applied, one is the heuristics method, and the other is the linear optimization method. By using these two approaches, the cost is minimized significantly from generation to consumer level. The energy storage

system (battery) is designed for efficient real-time operation for these EMS (See Fig. 11). Fig. 11 illustrates the output of energy measures, where microgrid voltage (V), output power (kW), ESS SOC (%), and electricity price (USD/kWh) will be displayed after the final result analysis. The traditional heuristic and optimization methods have existed inside the EMS in Fig. 11. Depending on the specific time of the day and condition of the battery, the EMS decides whether the battery should be charged, discharged, or idle. The state flow chart of the traditional heuristic method is shown in Fig. 12, where different states are represented in different boxes. Initially, the heuristic EMS observes the whole condition of the microgrid operation and then loads the energy data. This all depends on conditions like the time of the day and the SoC condition of the battery. After running the heuristic approach, the decision logic will show what is analyzed in the state flow chart step-by-step.

The operational flow of the linear programming optimization method is shown in the lower part of Fig. 11, which is more efficient compared with the heuristic method. This method is applied in problem-based optimization formulations to find out optimal decision variables. Initially, battery solar PV optimization logic is applied, which starts with constructing the problem. Then the variables are declared one by one, like solar PV system, power production, ESS from the grid, power from the battery, and energy from the battery condition. Some constraints are replaced, like load balance, which will also be declared. The main objective of this approach is to minimize the operating cost function. After that, energy optimization logic is applied, where every parameter is defined, like operating time, solar PV system power production (clear/cloudy day) data, solar PV system energy storage (clear/cloudy day) data, ESS condition, various load power data, and other integrated microgrid information. Then the linear optimization approach will show all the optimization results and cost minimization results graphically.

## 4. Result analysis, key findings and discussion

Daily solar irradiance data (clear day,  $Irra_{day(clear)}$  and cloudy day,  $Irra_{day(cloudy)}$  radiation) on an ideally inclined surface are utilized and examined to analyze the results since the measurement stations are optimally aligned (See Fig. 13(a)). The clear,  $P_{PV(clear)}$  and cloudy day,  $P_{PV(cloudy)}$  forecast PV power is represented in Fig. 13(b), which is calculated from eq (42) and eq (43), respectively. The various types of loads (residential, commercial, industrial, and others) are measured for the integrated microgrid system. The overall daily load duration curve is evaluated in Fig. 14.

$$P_{PV(clear)} = Irra_{day(clear)} \times A_{PV} \times \eta_{PV} \quad (42)$$

$$P_{PV(cloudy)} = Irra_{day(cloudy)} \times A_{PV} \times \eta_{PV} \quad (43)$$

The battery SoC energy constraints will be kept between 20% and 80% SoC, which will be good for battery health and life cycle. The initial battery energy,  $E_{max}$  is calculated by eq (44), where 50% SoC is assumed for the ideal condition. However, a lithium-ion battery is used in this suggested microgrid with the lowest 10% SoC energy so that the more stored energy will be possible to inject into the microgrid when needed. Battery Energy,  $Batt_{Energy} = Batt_{cap} \times 3.6 \times 10^6 = 2500 \text{ kWh} \times 3.6 \times 10^6 = 9 \times 10^9 \text{ W}$ , where the energy generated by a kW power source in 1 h is  $1 \text{ kWh} = 3.6 \times 10^6 \text{ Joule}$ . When, maximum power,  $P_{max}$  is around +400 kW then  $SoC_{max} = 80\%$  and minimum power,  $P_{min}$  is around -400 kW then  $SoC_{min} = 20\%$ .

$$E_{max} = SoC_{min,max} \times Batt_{Energy} \quad (44)$$

$$E_{max} = SoC_{max} \times Batt_{Energy} \quad (45)$$

$$E_{max} = SoC_{min} \times Batt_{Energy} \quad (46)$$

Daily basis analysis is analyzed and evaluated for an integrated

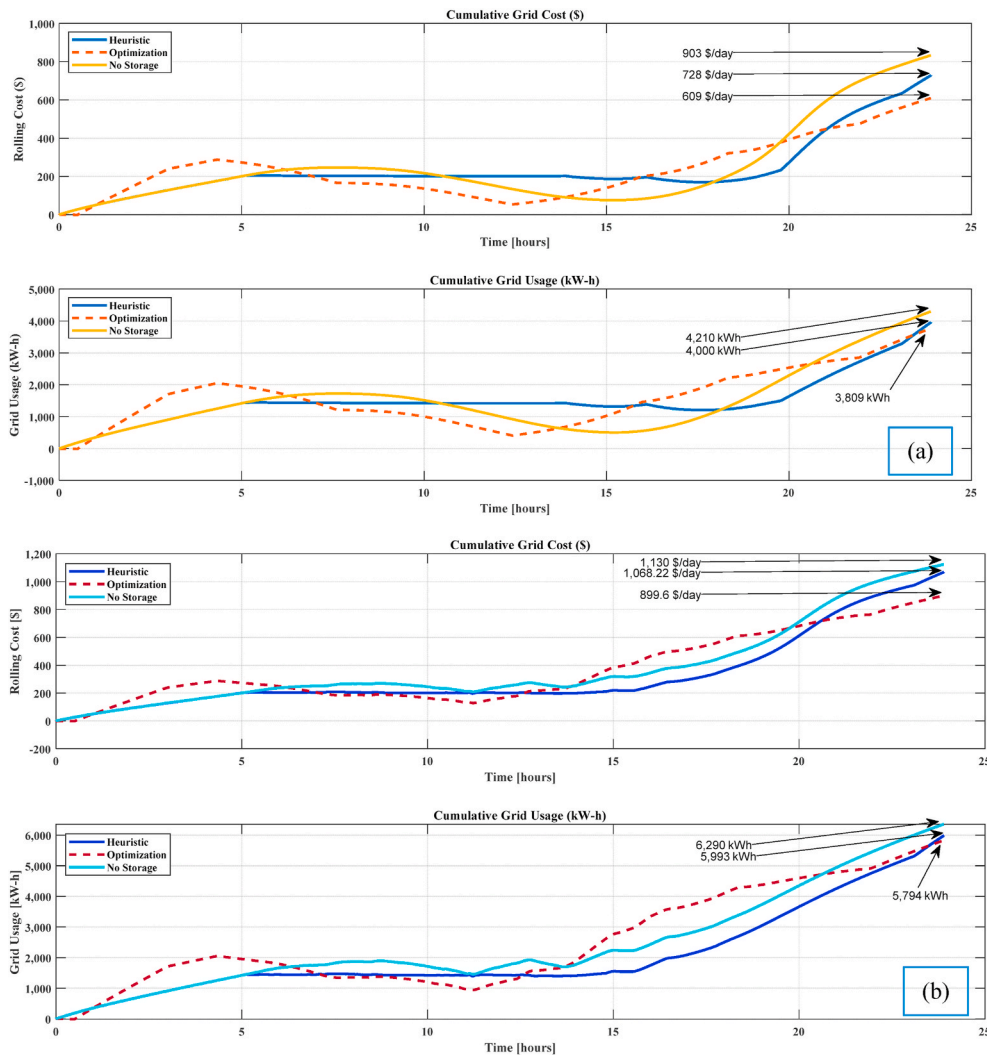


Fig. 18. Comparison of cumulative grid cost and grid usage for heuristic and optimization approach (a) clear, (b) cloudy day.

Table 4

Comparison of day basis total cost and usage of grid electricity.

Day (Weather)	Grid cost per day retail (\$)			% Of cost savings LP optimization over Heuristic	Grid usage per day retail (kWh)			% Of cost savings LP optimization over Heuristic
	Without EMS	Heuristic	LP Optimization		Without EMS	Heuristic	LP Optimization	
Clear (Sunny)	903.2	728.0	609.1	19.53	4,210.1	4,000.3	3,809.4	5.01
Cloudy (Rainy)	1,130.0	1,068.3	899.1	19.01	6,290.4	5,993.2	5,794.1	3.44

microgrid system for optimal EMS. The number of consecutive few days of data is evaluated for optimization factors. The time step for heuristic and LP optimization operations is set to a one-day scale (one day or 24 h or 1440 min or 86,400 s).

The heuristic technique employing state flow (chart flow) EMS is applied in the solar PV/battery-based integrated microgrid. Fig. 15 demonstrate the EMS heuristic method outcomes for a clear day and a cloudy day. The microgrid voltage (RMS value), solar PV power, ESS power, grid power, and various load power curves are investigated. The minimum and maximum ranges of the ESS SoC are also investigated. The anticipated grid pricing values (cents/kWh), which vary with load demand, are determined. Because the peak of the ESS and SoC is not correct when solar power is available, the energy price rate (consumer energy rate) is relatively high in this technique, which is not consumer-

friendly.

The battery and solar system optimization function is used to optimize the ESS usage for the integrated microgrid. The optimization method based on a linear programming approach minimizes the cost of the power from the grid while meeting the load with power from solar PV, battery, and grid. It will help to minimize the cost of electricity from the grid. The battery's power input and output from solar PV, grid power, battery state, and load demand are calculated from eq (47). The linear programming optimization routine takes the current state of the battery, battery energy (nominal charge), optimization time data, and the output data of the forecast algorithm like cost values, solar PV power, and load power for its operation, as shown in Figs. 7 and 11. Then, optimal linear programming energy management logic is applied. The output of this logic is optimized power output, which can run



supplied back to the model. It will run at different times for different forecast profiles. The power electronics components are typically running in minimal time steps, and the optimization is much slower on a second-time scale. The linear optimization approach results of the EMS are illustrated in Fig. 16. With this method, the electricity price rate is significantly reduced compared with heuristic methods. The peak of the ESS and SoC is found to be significant when solar power is available, which is consumer-friendly. For the sunny day optimization, as shown in Fig. 16(a). Initially, the battery responds to soft pecks with varying demand and price data. The battery gets charged and dis-charged accordingly with the solar power availability. The linear optimization system quickly evaluates the charge and discharge state for different circumstances. As presented in Fig. 16(b), a fluctuation of solar PV power is found for cloudy day optimization due to the rainy season. Here, the battery is found to be dependent on the demand and price of electricity.

$$P_{pv}(k) + P_{grid}(k) + P_{bat}(k) = P_{load}(k) \quad (47)$$

The overall output of the linear programming optimization function is the battery power, grid price, and load demand balance, which is defined in Fig. 17. The optimum demand-side management relates to the battery power command. This is probably the effect of the system on how the battery will operate. So, voltages and low power frequencies might fluctuate. It is possibly a good idea and probably helpful to see the optimization's impact on the command. This optimization approach ensures that it does not cause any harm to the entire EMS. On the top graph, ESS optimization is done over time (kWh), then grid pricing (USD/kWh), and power (W) from the solar PV system, battery bank, integrated microgrid, and various load demands is measured. With this method, the terms of demand response can be predicted. The optimization logic gives a command to pre-charge the battery while running in the higher demand phase and then dis-charge accordingly. With this technique, the local demand is reduced from the microgrid, thereby reducing the total system cost. The optimization method also controls the market price based on the energy demand of baseload and peak load. At the bottom of the graph, the output power of the ESS and trading power with the microgrid sharply fluctuate from daytime (morning, 8 a. m. to noon, 2 p.m.) because of battery charging from the solar PV system. The optimal ESS covers the grid energy balance from 1 to 18 h in a day. Due to the lowest SoC condition of ESS, the 18-h to 22-h time zone is the peak load demand hours. During peak hours, electricity is injected from the central grid to the microgrid area to balance the peak hour load demands. So, electricity prices are at their highest during peak hours.

The operations of the heuristic EMS in the integrated microgrid system are solely based on market mechanisms. This model does not include the impact of intermittent solar systems or the volatility of market costs. Furthermore, the best LP EMS actions are determined by the actual market value, trading power value, intermittent solar system, and microgrid surplus/shortage amount. This optimization method also considers the uncertainties of surplus and shortage of electricity in the microgrid. The unpredictability of load demand and the solar PV system in the microgrid is also evaluated. As a result, the suggested LP optimization EMS can cope with system uncertainties in both grid-connected and islanded modes. The electricity price for the various consumer categories of the integrated microgrid system is highlighted in Table 3.

For the sunny day, the heuristic and the linear optimization approach cost per day is calculated to be 728.0 and 609.1 USD, respectively, as illustrated in Fig. 18(a). For the cloudy day, the heuristic and the linear optimization approach cost per day is calculated to be 1,068.3 and 899.1 USD, respectively, as shown in Fig. 18(b). Finally, comparing results with this traditional heuristic and optimization-based methods is evaluated in Fig. 18. For the heuristic approach, the result will be going to depend on how the heuristic logic parameter responds to the demand, load, and various cost data. However, the forecast data will be predictable quite well concerning time response for the linear optimization approach. Using the linear programming optimization approach will be

more flexible with loads and give a better demand response. Therefore, the operating cost will be significantly minimized. Table 4 shows the cumulative off-grid cost (USD) and cumulative grid usage (kWh) projection. The optimization approach reduces both the cost and grid usage, respectively, compared to the heuristic approach. If there is a no-storage option applied, the grid cost is found to be the highest. Then, if there is a traditional heuristic approach applied, the grid cost is found to be reduced. However, in the case of the linear optimization approach applied, the grid cost was found to be the lowest. The highest rate accounted for the no-storage option in actual grid usage. Besides, the heuristic and optimization approaches are almost the same for actual grid usage. The optimization approach has given an extra advantage compared with the heuristic approach in almost every measure. The total cost of variable-priced electricity is calculated in \$/kWh. In the heuristic approach, the EMS cost is found to be \$728.0 for sunny days and \$1068.3 for cloudy days. While in the optimization approach, the EMS cost is found to be \$609.1 for a sunny day and \$899.1 for a cloudy day.

$$\begin{aligned} \text{Difference (\%)} &= \frac{\text{Input} - \text{Output}}{\text{Input}} \times 100\% \\ &= \frac{\text{Optimization} - \text{Heuristic}}{\text{Optimization}} \times 100\% \end{aligned} \quad (48)$$

In percentage, the difference between the two methods is calculated to be 19.53% of the cost with a 5.01% grid usage energy savings for a clear day and -19.01% of the cost with a 3.44% grid usage energy savings for cloudy days. Compared with the traditional heuristic method, the linear optimization method saved almost 19% in electricity prices and more than 3.44% in grid energy usage.

In summary, the advantages of this proposed LP optimization EMS in solar/battery-based integrated microgrid systems are as follows. The system significantly reduces losses and continuously monitors power-sharing in demand-side management. The microgrid's energy efficiency substantially increases. The proposed model reduces microgrid inside and outside grid energy usage. Electricity outage durations are reduced by proper management of power balancing and sharing. During peak period operation, it optimizes transformer loading. Thus, it improves interconnected grid network operations. Overall, it increases customer satisfaction and encourages more customers in self-driven EMS.

## 5. Conclusion and outlook

The main purpose of this research study is to minimize the total cost of variably priced electricity. The optimization approach based on linear programming (LP) is easy to implement, analyze, and evaluate the performance and has little computation complexity. The suggested optimum LP approach overcomes different types of limitations compared with the traditional heuristic approach. The whole process is used to develop the linear optimization routine that predicts forecast pricing and loading conditions that optimally store or sell energy from a grid-scale battery system. The simulation results clearly show that the LP-based optimization approach is cost-efficient. Using this optimization method, the cost of variable-priced electricity is 19% less when compared to heuristic state machine logic. The LP optimization also reduces the extra grid energy usage by around 3.44-5.01%. In the future, this research study will investigate the performance of constrained LP-based optimization approaches for more complex nonlinear and binary energy management problems. The focus will be given to reducing the dimensionality of the decision variables of the proposed LP-based optimization EMS. Furthermore, the microgrid's current model precision will be improved by adding the miles parameter and the element into the microgrid configuration.

## Declaration of competing interest

The authors declare that they have no known competing financial interests or personal relationships that could have appeared to influence the work reported in this paper.

## References

- Aghdam, F.H., Ghaemi, S., Kalantari, N.T., 2018. Evaluation of loss minimization on the energy management of multi-microgrid based smart distribution network in the presence of emission constraints and clean productions. *J. Clean. Prod.* 196, 185–201. <https://doi.org/10.1016/j.jclepro.2018.06.023>.
- Aghdam, F.H., Taghizadeh Kalantari, N., Mohammadi-Ivatloo, B., 2020. A stochastic optimal scheduling of multi-microgrid systems considering emissions: a chance constrained model. *J. Clean. Prod.* 275, 122965. <https://doi.org/10.1016/j.jclepro.2020.122965>.
- Ahmadi, S.E., Rezaei, N., 2020. A new isolated renewable based multi microgrid optimal energy management system considering uncertainty and demand response. *Int. J. Electr. Power Energy Syst.* 118, 105760. <https://doi.org/10.1016/j.ijepes.2019.105760>.
- Allouhi, A., Saadani, R., Buker, M.S., Kousksou, T., Jamil, A., Rahmoune, M., 2019. Energetic, economic and environmental (3E) analyses and LCOE estimation of three technologies of PV grid-connected systems under different climates. *Sol. Energy* 178, 25–36. <https://doi.org/10.1016/j.solener.2018.11.060>.
- Bansal, N., Jaiswal, S.P., Singh, G., 2021. Comparative investigation of performance evaluation, degradation causes, impact and corrective measures for ground mount and rooftop solar PV plants – a review. *Sustain. Energy Technol. Assessments* 47, 101526. <https://doi.org/10.1016/j.seta.2021.101526>.
- Bellido, M.H., Rosa, L.P., Pereira, A.O., Falcão, D.M., Ribeiro, S.K., 2018. Barriers, challenges and opportunities for microgrid implementation: the case of Federal University of Rio de Janeiro. *J. Clean. Prod.* 188, 203–216. <https://doi.org/10.1016/j.jclepro.2018.03.012>.
- Bui, V.-H., Hussain, A., Kim, H.-M., 2018. A multiagent-based hierarchical energy management strategy for multi-microgrids considering adjustable power and demand response. *IEEE Trans. Smart Grid* 9, 1323–1333. <https://doi.org/10.1109/TSG.2016.2585671>.
- Bui, V.H., Hussain, A., Im, Y.H., Kim, H.M., 2019. An internal trading strategy for optimal energy management of combined cooling, heat and power in building microgrids. *Appl. Energy* 239, 536–548. <https://doi.org/10.1016/j.apenergy.2019.01.160>.
- Bui, V.H., Hussain, A., Kim, H.M., 2020. Double Deep Q -Learning-Based distributed operation of battery energy storage system considering uncertainties. *IEEE Trans. Smart Grid* 11, 457–469. <https://doi.org/10.1109/TSG.2019.2924025>.
- Cao, Y., Zhou, B., Or, S.W., Chan, K.W., Liu, N., Zhang, K., 2021. An interactive tri-level multi-energy management strategy for heterogeneous multi-microgrids. *J. Clean. Prod.* 319, 128716. <https://doi.org/10.1016/j.jclepro.2021.128716>.
- Chaouachi, A., Kamel, R.M., Andoulsi, R., Nagasaka, K., 2013. Multiobjective intelligent energy management for a microgrid. *IEEE Trans. Ind. Electron.* 60, 1688–1699. <https://doi.org/10.1109/TIE.2012.2188873>.
- Chen, W., Shao, Z., Wakil, K., Aljojo, N., Samad, S., Rezvani, A., 2020. An efficient day-ahead cost-based generation scheduling of a multi-supply microgrid using a modified krill herd algorithm. *J. Clean. Prod.* 272, 122364. <https://doi.org/10.1016/j.jclepro.2020.122364>.
- Cortés, P., Auladell-León, P., Muñozuri, J., Onieva, L., 2020. Near-optimal operation of the distributed energy resources in a smart microgrid district. *J. Clean. Prod.* 252. <https://doi.org/10.1016/j.jclepro.2019.119772>.
- Daneshvar, M., Mohammadi-Ivatloo, B., Asadi, S., Anvari-Moghaddam, A., Rasouli, M., Abapour, M., et al., 2020. Chance-constrained models for transactive energy management of interconnected microgrid clusters. *J. Clean. Prod.* 271, 122177. <https://doi.org/10.1016/j.jclepro.2020.122177>.
- De, M., Das, G., Mandal, K.K., 2021. An effective energy flow management in grid-connected solar-wind-microgrid system incorporating economic and environmental generation scheduling using a meta-dynamic approach-based multiobjective flower pollination algorithm. *Energy Rep.* 7, 2711–2726. <https://doi.org/10.1016/j.egy.2021.04.006>.
- Dey, B., Bhattacharyya, B., Márquez, F.P.G., 2021. A hybrid optimization-based approach to solve environment constrained economic dispatch problem on microgrid system. *J. Clean. Prod.* 307. <https://doi.org/10.1016/j.jclepro.2021.127196>.
- Dubarry, M., Baure, G., Pastor-Fernández, C., Yu, T.F., Widanage, W.D., Marco, J., 2019. Battery energy storage system modeling: a combined comprehensive approach. *J. Energy Storage* 21, 172–185. <https://doi.org/10.1016/j.est.2018.11.012>.
- Fathima, A.H., Palanisamy, K., 2015. Optimization in microgrids with hybrid energy systems – a review. *Renew. Sustain. Energy Rev.* 45, 431–446. <https://doi.org/10.1016/j.rser.2015.01.059>.
- Gazijehani, F.S., Ajoulabadi, A., Ravadanegh, S.N., Salehi, J., 2020. Joint energy and reserve scheduling of renewable powered microgrids accommodating price responsive demand by scenario: a risk-based augmented epsilon-constraint approach. *J. Clean. Prod.* 262. <https://doi.org/10.1016/j.jclepro.2020.121365>.
- Gomes, L., Spínola, J., Vale, Z., Corchado, J.M., 2019. Agent-based architecture for demand side management using real-time resources' priorities and a deterministic optimization algorithm. *J. Clean. Prod.* 241. <https://doi.org/10.1016/j.jclepro.2019.118154>.
- Gong, X., Dong, F., Mohamed, M.A., Awwad, E.M., Abdullah, H.M., Ali, Z.M., 2020. Towards distributed based energy transaction in a clean smart island. *J. Clean. Prod.* 273, 122768. <https://doi.org/10.1016/j.jclepro.2020.122768>.
- Gulagi, A., Ram, M., Solomon, A.A., Khan, M., Breyer, C., 2020. Current energy policies and possible transition scenarios adopting renewable energy: a case study for Bangladesh. *Renew. Energy* 155, 899–920. <https://doi.org/10.1016/j.renene.2020.03.119>.
- Jordehi, A.R., Javadi, M.S., Catalão, J.P.S., 2020a. Energy management in microgrids with battery swap stations and var compensators. *J. Clean. Prod.* 272, 122943. <https://doi.org/10.1016/j.jclepro.2020.122943>.
- Jordehi, A.R., Javadi, M.S., Catalão, J.P.S., 2020b. Energy management in microgrids with battery swap stations and var compensators. *J. Clean. Prod.* 272, 1–32. <https://doi.org/10.1016/j.jclepro.2020.122943>.
- Kermani, M., Adelmanesh, B., Shirdare, E., Sima, C.A., Carni, D.L., Martirano, L., 2021. Intelligent energy management based on SCADA system in a real Microgrid for smart building applications. *Renew. Energy* 171, 1115–1127. <https://doi.org/10.1016/j.renene.2021.03.008>.
- Kumar, P.S., Chandrasena, R.P.S., Ramu, V., Srinivas, G.N., Babu, K.V.S.M., 2020. Energy management system for small scale hybrid wind solar battery based microgrid. *IEEE Access* 8, 8336–8345. <https://doi.org/10.1109/ACCESS.2020.2964052>.
- Kumar, R.S., Raghav, L.P., Raju, D.K., Singh, A.R., 2021. Intelligent demand side management for optimal energy scheduling of grid connected microgrids. *Appl. Energy* 285, 116435. <https://doi.org/10.1016/j.apenergy.2021.116435>.
- Lee, A., Zinaman, O., Logan, J., Bazilian, M., Arent, D., Newmark, R.L., 2012. Interactions, complementarities and tensions at the nexus of natural gas and renewable energy. *Electr. J.* 25, 38–48. <https://doi.org/10.1016/j.tej.2012.10.021>.
- Lee, E.K., Shi, W., Gadh, R., Kim, W., 2016. Design and implementation of a microgrid energy management system. *Sustain. Times* 8, 1–19. <https://doi.org/10.3390/su8111143>.
- Li, C., Jia, X., Zhou, Y., Li, X., 2020. A microgrids energy management model based on multi-agent system using adaptive weight and chaotic search particle swarm optimization considering demand response. *J. Clean. Prod.* 262, 121247. <https://doi.org/10.1016/j.jclepro.2020.121247>.
- Li, W., Cui, H., Nemeth, T., Jansen, J., Ünlübayir, C., Wei, Z., et al., 2021. Deep reinforcement learning-based energy management of hybrid battery systems in electric vehicles. *J. Energy Storage* 36, 102355. <https://doi.org/10.1016/j.est.2021.102355>.
- Li, W., Rentemeister, M., Badedo, J., Jöst, D., Schulte, D., Sauer, D.U., 2020. Digital twin for battery systems: cloud battery management system with online state-of-charge and state-of-health estimation. *J. Energy Storage* 30, 101557. <https://doi.org/10.1016/j.est.2020.101557>.
- Mansouri, S.A., Ahmarinejad, A., Nematbakhsh, E., Javadi, M.S., Jordehi, A.R., Catalão, J.P.S., 2021. Energy management in microgrids including smart homes: a multi-objective approach. *Sustain. Cities Soc.* 69, 102852. <https://doi.org/10.1016/j.scs.2021.102852>.
- Marzband, M., Azarnejadian, F., Savaghebi, M., Guerrero, J.M., 2017. An optimal energy management system for islanded microgrids based on multiperiod artificial bee colony combined with Markov chain. *IEEE Syst. J.* 11, 1712–1722. <https://doi.org/10.1109/JYST.2015.2422253>.
- Michaelson, D., Mahmood, H., Jiang, J., 2017. A predictive energy management system using pre-emptive load shedding for islanded photovoltaic microgrids. *IEEE Trans. Ind. Electron.* 64, 5440–5448. <https://doi.org/10.1109/TIE.2017.2677317>.
- Moazeni, F., Khazaei, J., 2020. Optimal operation of water-energy microgrids; a mixed integer linear programming formulation. *J. Clean. Prod.* 275, 122776. <https://doi.org/10.1016/j.jclepro.2020.122776>.
- Mosa, M.A., Ali, A.A., 2021. Energy management system of low voltage dc microgrid using mixed-integer nonlinear programming and a global optimization technique. *Electr. Power Syst. Res.* 192, 106971. <https://doi.org/10.1016/j.epr.2020.106971>.
- Nagapurkar, P., Smith, J.D., 2019. Techno-economic optimization and social costs assessment of microgrid-conventional grid integration using genetic algorithm and Artificial Neural Networks: a case study for two US cities. *J. Clean. Prod.* 229, 552–569. <https://doi.org/10.1016/j.jclepro.2019.05.005>.
- Naik, K.R., Rajpathak, B., Mitra, A., Kolhe, M.L., 2021. Adaptive energy management strategy for sustainable voltage control of PV-hydro-battery integrated DC microgrid. *J. Clean. Prod.* 315, 128102. <https://doi.org/10.1016/j.jclepro.2021.128102>.
- Rabiee, A., Sadeghi, M., Aghaei, J., 2018. Modified imperialist competitive algorithm for environmental constrained energy management of microgrids. *J. Clean. Prod.* 202, 273–292. <https://doi.org/10.1016/j.jclepro.2018.08.129>.
- Rahim, S., Javadi, N., Khan, R.D., Nawaz, N., Iqbal, M., 2019. A convex optimization based decentralized real-time energy management model with the optimal integration of microgrid in smart grid. *J. Clean. Prod.* 236, 117688. <https://doi.org/10.1016/j.jclepro.2019.117688>.
- Robert, F.C., Sisodia, G.S., Gopalan, S., 2018. A critical review on the utilization of storage and demand response for the implementation of renewable energy microgrids. *Sustain. Cities Soc.* 40, 735–745. <https://doi.org/10.1016/j.scs.2018.04.008>.
- Sachs, J., Sawodny, O., 2016. A two-stage model predictive control strategy for economic diesel-PV-battery island microgrid operation in rural areas. *IEEE Trans. Sustain. Energy* 7, 903–913. <https://doi.org/10.1109/TSTE.2015.2509031>.
- Sahoo, S.K., Sinha, A.K., Kishore, N.K., 2018. Control techniques in AC, DC, and hybrid AC-DC microgrid: a review. *IEEE J. Emerg. Sel. Top Power Electron.* 6, 738–759. <https://doi.org/10.1109/JESTPE.2017.2786588>.
- Sedighzadeh, M., Doyran, R.V., Rezazadeh, A., 2020. Optimal Simultaneous Allocation of Passive Filters and Distributed Generations as Well as Feeder Reconfiguration to Improve Power Quality and Reliability in Microgrids, vol. 265. Elsevier Ltd. <https://doi.org/10.1016/j.jclepro.2020.121629>.

- Shehzad Hassan, M.A., Chen, M., Lin, H., Ahmed, M.H., Khan, M.Z., Chughtai, G.R., 2019. Optimization modeling for dynamic price based demand response in microgrids. *J. Clean. Prod.* 222, 231–241. <https://doi.org/10.1016/j.jclepro.2019.03.082>.
- Shiva Kumar, B., Sudhakar, K., 2015. Performance evaluation of 10 MW grid connected solar photovoltaic power plant in India. *Energy Rep.* 1, 184–192. <https://doi.org/10.1016/j.egy.2015.10.001>.
- da Silva, I.R.S., de Rabelo, R.A.L., Rodrigues, J.J.P.C., Solic, P., Carvalho, A., 2020. A preference-based demand response mechanism for energy management in a microgrid. *J. Clean. Prod.* 255 <https://doi.org/10.1016/j.jclepro.2020.120034>.
- Singh, P., Lather, J.S., 2021. Power management and control of a grid-independent DC microgrid with hybrid energy storage system. *Sustain. Energy Technol. Assessments* 43, 100924. <https://doi.org/10.1016/j.seta.2020.100924>.
- Sukumar, S., Mokhlis, H., Mekhilef, S., Naidu, K., Karimi, M., 2017. Mix-mode energy management strategy and battery sizing for economic operation of grid-tied microgrid. *Energy* 118, 1322–1333. <https://doi.org/10.1016/j.energy.2016.11.018>.
- Tabar, V.S., Jirdehi, M.A., Hemmati, R., 2018. Sustainable planning of hybrid microgrid towards minimizing environmental pollution, operational cost and frequency fluctuations. *J. Clean. Prod.* 203, 1187–1200. <https://doi.org/10.1016/j.jclepro.2018.05.059>.
- Tang, S., Jiang, M., Abbassi, R., Jerbi, H., latifi, M., 2021. A cost-oriented resource scheduling of a solar-powered microgrid by using the hybrid crow and pattern search algorithm. *J. Clean. Prod.* 313, 127853. <https://doi.org/10.1016/j.jclepro.2021.127853>.
- Tete, P.R., Gupta, M.M., Joshi, S.S., 2021. Developments in battery thermal management systems for electric vehicles: a technical review. *J. Energy Storage* 35, 102255. <https://doi.org/10.1016/j.est.2021.102255>.
- Wang, C., Zhang, Z., Abedinia, O., Farkoush, S.G., 2021. Modeling and analysis of a microgrid considering the uncertainty in renewable energy resources, energy storage systems and demand management in electrical retail market. *J. Energy Storage* 33, 102111. <https://doi.org/10.1016/j.est.2020.102111>.
- Xie, C., Wang, D., Lai, C.S., Wu, R., Wu, X., Lai, L.L., 2021. Optimal sizing of battery energy storage system in smart microgrid considering virtual energy storage system and high photovoltaic penetration. *J. Clean. Prod.* 281, 125308. <https://doi.org/10.1016/j.jclepro.2020.125308>.
- Yang, F., Feng, X., Li, Z., 2019. Advanced microgrid energy management system for future sustainable and resilient power grid. *IEEE Trans. Ind. Appl.* 55, 7251–7260. <https://doi.org/10.1109/TIA.2019.2912133>.
- Yassuda Yamashita, D., Vechiu, I., Gaubert, J.-P., 2021. Two-level hierarchical model predictive control with an optimised cost function for energy management in building microgrids. *Appl. Energy* 285, 116420. <https://doi.org/10.1016/j.apenergy.2020.116420>.
- Zhang, L., Yang, Y., Li, Q., Gao, W., Qian, F., Song, L., 2021. Economic optimization of microgrids based on peak shaving and CO2 reduction effect: a case study in Japan. *J. Clean. Prod.* 321, 128973. <https://doi.org/10.1016/j.jclepro.2021.128973>.
- Zia, M.F., Elbouchikhi, E., Benbouzid, M., 2018. Microgrids energy management systems: a critical review on methods, solutions, and prospects. *Appl. Energy* 222, 1033–1055. <https://doi.org/10.1016/j.apenergy.2018.04.103>.